



저작자표시-비영리-변경금지 2.0 대한민국

이용자는 아래의 조건을 따르는 경우에 한하여 자유롭게

- 이 저작물을 복제, 배포, 전송, 전시, 공연 및 방송할 수 있습니다.

다음과 같은 조건을 따라야 합니다:



저작자표시. 귀하는 원저작자를 표시하여야 합니다.



비영리. 귀하는 이 저작물을 영리 목적으로 이용할 수 없습니다.



변경금지. 귀하는 이 저작물을 개작, 변형 또는 가공할 수 없습니다.

- 귀하는, 이 저작물의 재이용이나 배포의 경우, 이 저작물에 적용된 이용허락조건을 명확하게 나타내어야 합니다.
- 저작권자로부터 별도의 허가를 받으면 이러한 조건들은 적용되지 않습니다.

저작권법에 따른 이용자의 권리는 위의 내용에 의하여 영향을 받지 않습니다.

이것은 [이용허락규약\(Legal Code\)](#)을 이해하기 쉽게 요약한 것입니다.

[Disclaimer](#)

Master's Thesis
석사 학위논문

The study of sensor structure to perceive a surface
texture for psychological tactile sensor

Kwonsik Shin (신 권 식 申 權 湜)

Department of Information and Communication Engineering

정보통신융합공학전공

DGIST

2017

The study of sensor structure to perceive a surface texture for psychological tactile sensor

Advisor : Professor Jae Eun Jang

Co-advisor : Professor Seong-Woon Yu

By

Kwonsik Shin

Department of Information and Communication Engineering

DGIST

A thesis submitted to the faculty of DGIST in partial fulfillment of the requirements for the degree of Master of Science in the Department of Information and Communication Engineering. The study was conducted in accordance with Code of Research Ethics¹

01. 04. 2017

Approved by

Professor Jae Eun Jang (Signature)
(Advisor)

Professor Seong-Woon Yu (Signature)
(Co-Advisor)

¹ Declaration of Ethical Conduct in Research: I, as a graduate student of DGIST, hereby declare that I have not committed any acts that may damage the credibility of my research. These include, but are not limited to: falsification, thesis written by someone else, distortion of research findings or plagiarism. I affirm that my thesis contains honest conclusions based on my own careful research under the guidance of my thesis advisor.

The study of sensor structure to perceive a surface texture for psychological tactile sensor

Kwonsik Shin

Accepted in partial fulfillment of the requirements for the degree of Master of Science

01. 04. 2017

Head of Committee 장 재 은 (인)

Prof. Jae Eun Jang

Committee Member 유 성 운 (인)

Prof. Seong-Woon Yu

Committee Member 최 지 응 (인)

Prof. Ji-Woong Choi

Abstract

Tactile sensors mimicking the sense of touch of the human have been studied gradually and various technologies sensing an external stimulus have been suggested as well. The human detects some external physical stimuli and generates psychological feeling such as roughness, softness or pain through the touch. Since people have different criteria for the psychological feelings, there are a lot of issues as to which components are most informative for perceiving the parameters. To give these psychological feelings to artificial system as like android robot or smart phone, sensing a surface texture is one of the most informative perception among various physical parameters. Sensing a surface texture also has many issues since many kinds of factors such as vibration, strain and friction should be considered to detect the surface texture. Robotic fingers applied a contact point analysis, feedback loop and flow chart are used for a surface texture detection in robot field. However, those methods should need complex algorithm and programming to analyze data concerning a surface texture from the robotic fingers. In this paper, a piezoelectric type array sensor structure was demonstrated with sliding mechanism to restore a surface texture precisely as like human. The suggested array sensor design with excellent dynamic response of piezoelectric material gave a higher spatial resolution detection than the resolution of sensor system and detected sliding velocity, essential parameter to restore surface texture from electrical signal, as well. The sensor could calculate various sliding velocities from 10mm/s to 70mm/s accurately by simple electrical signal analysis produced from sensor arrays. A soft material was applied for the sensor to enhance surface detection ability and it allowed that the array sensor could distinguish between a spike type and a doom type shape. Signal processing was optimized and simplified for a surface texture restoration. Restored surface textures had high accuracy compared with real texture structures and color mapping skill was applied for the restored textures images to express the pattern of texture. The capabilities of velocity detecting and texture restoration allow the sensor can be utilized to electro-mechanical systems as the physical and the psychological tactile sensor.

Keywords: Piezoelectric, Array structure, Psychological, PVDF-TrFE, Surface texture, Tactile sensor;

List of Contents

Abstract.....	i
List of contents.....	ii
List of tables.....	iv
List of figures.....	v

I . INTRODUCTION

1.1 Overview.....	1
1.2 Motivation.....	3
1.3 Thesis Overview.....	4

II . BACKGROUNDS

2.1 Human Tactile System.....	5
2.1.1 Tactile Receptors.....	5
2.1.2 Nervous System of Touch.....	7
2.2 Surface Textures.....	8
2.3 Previous Works for Sensing Surface Textures.....	9
2.3.1 Friction.....	9
2.3.2 Roughness.....	10
2.3.3 Vibration.....	11
2.3.4 Optical Sensor.....	11
2.3.5 Piezophotonic Sensor.....	12

III. EXPERIMENT DETAILS

3.1 Piezo Sensor Array.....	13
3.1.1 Principal of Piezoelectricity.....	14
3.1.2 Piezoelectric Materials.....	17
3.1.3 Array Structure.....	19
3.1.4 Soft Materials.....	19
3.2 Fabrication and Structure of Piezo Sensor Array.....	20
3.3 Design of Textures.....	24
3.4 Experimental Setup.....	25

IV. RESULTS AND DISCUSSION

4.1 Characteristics of Piezo Sensor Array.....	27
4.1.1 Touch Experiment.....	27
4.1.2 Sliding Experiment.....	28
4.2 Characteristics of Sliding Signals.....	32
4.2.1 Signal Difference depending on Texture Shapes.....	32
4.2.2 Signal Difference depending on Weights.....	34
4.2.3 Signal Difference depending on Velocity.....	34

4.3 Sliding Velocity & Texture's Pitch Calculation	35
4.4 Texture Restoration.....	38
4.5 Resolution of the Piezo Sensor Array	40
4.6 Characteristics of Piezo Sensor Array applied Soft Material.....	41
4.6.1 Sliding Signal Changes	42
4.6.2 Texture Restoration	43
V. CONCLUSION	45

List of tables

Table 4.1.2.1. Correlation coefficients between bump, spike and dome signals. ·	
.....	31

List of figures

Fig 1.1.1. Schematic of sensing process.	1
Fig 1.2.1. Images of touch and sliding sensing method	4
Fig 2.1.1.1. Characteristics and stimulus responses of mechanoreceptors	6
Fig 2.1.2.1. The dorsal column-medial lemniscal pathway	7
Fig 2.2.1. AFM mechanism and scanning image	8
Fig 3.1.1.1. The piezoelectric effect mechanism	15
Fig 3.1.1.2 Relations among electrical and mechanical quantities	16
Fig 3.2.1 Schematic of the top layer fabrication process	21
Fig 3.2.2 Schematic of the bottom layer fabrication process.....	22
Fig 3.2.3 Schematic of the piezo sensor array set-up	23
Fig 3.2.4 Optical images of the top layer of piezo sensor array	23
Fig 3.3.1 Enlarged textures designs of the bump, spike and dome shapes	24
Fig 3.3.2 Optical image of the three different textures	25
Fig 3.4.1 Experimental set-up image of linear stage with weight container and texture stage	26
Fig 3.4.2 Mounted the bump texture to the texture stage.....	26
Fig 4.1.1.1 The results of touch experiment with various textures	28
Fig 4.1.2.1. Image of sliding experimental setup with leaner stage	29
Fig 4.1.2.2. Sliding signals of the different textures from the sensor array	29
Fig 4.1.2.3. A signal matching graph applied correlation signal processing	31
Fig 4.2.1.1. Sliding signal analysis in 30mm/s condition.....	33
Fig 4.2.2.1. Sliding signal changes according to weight and velocity	35
Fig 4.3.1. Velocity and pitch calculation processes using sliding signals	37
Fig 4.4.1. Texture restoration of the three different textures	39
Fig 4.5.1. Sliding signal of random pitch in 35mm/s condition	40
Fig 4.6.1.1. A deformation mechanism and signal changes after applying soft material to the sensor.....	41
Fig 4.6.2.1. Texture restoration applied a soft material	43

I. INTRODUCTION

1.1 Overview

The five senses of human have been an interesting study from long time ago. Studies about sight and hearing have been studied, but the sense of touch has still a lot of issues relatively compared with sight and hearing. The sense of touch is quite related with various external stimuli such as pressure, temperature, vibration, tension, shear force and so on. Many kinds of tactile receptors are responded respectively to the external stimuli and then make an electrical signal called the action potential [1]. The tactile perceptions are performed by various kinds of receptors interacting with the human nervous system [2]. The electrical signals are sent to the human nervous system, so that human is able to percept the sense of touch finally [56]. Recently, some groups have been studying about sensors mimicking the tactile receptors. For example, capacitive [3] [4] [5], piezoelectric

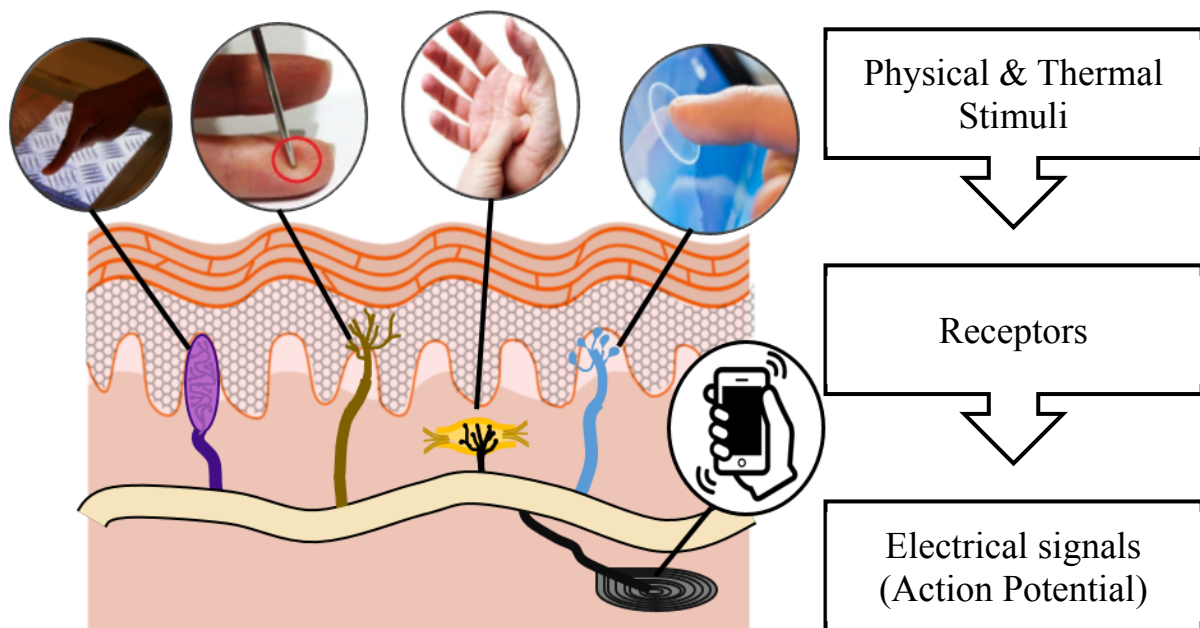


Fig 1.1.1. Schematic of sensing process. Tactile receptors generate electrical signals which is called the action potential due to external stimuli

[6] [7] [8], piezoresistive [9] [10] and pyroelectric [11] [12] type sensors have been studied to detect pressure and temperature and these types of sensors are able to conduct as the mechanoreceptors and thermoreceptors. Various sensor structures are also considered for sensitivity, high resolution, multi touch as well as flexibility and stretchability. However, artificial tactile sensors cannot perfectly cover the sense of human touch yet because the human feels not only external physical stimuli such as pressure and temperature but also psychological parameters such as roughness, hardness, softness and pain through the touch. Among these psychological feeling, a roughness and a softness are one of the most difficult mimicking functions, since people have different criteria for sensing the psychological parameters and there are a lot of issues as to which physical components are most informative for perceiving the parameters. However, it is an indisputable factor that sensing a surface texture is starting point to percept those 'roughness and softness feeling'. Unfortunately, it is rare to find a studying results of tactile sensor related with a surface texture detection in comparison with pressure and temperature detection. One of reasons is that there is no consensus as to which mechanism of strain is most informative for texture sensing[13]. Normally, human can feel the surface texture by sliding finger on a surface of object. At that time, shear force, friction, vibration and contact area are changed continuously depending on the morphology of the surface texture during the sliding. So many kinds of factors should be considered to detect the surface texture compared with pressure and temperature[13]. A robotic finger applied contact point analysis[14], feedback loop[15] [16], flow chart[17], Gaussian statistics[18] method have been proposed for a surface texture detection in robot field. However, the methods should need complex algorithm and programming for measuring surface information from the robotic finger. Also most robotic finger consists of a unit sensor, so that coefficient and constant factors should be known in advance for

analyzing surface textures. A piezophotonic and optical sensors are sometimes used for a surface texture sensing but the sensors should require a light source and additional optical equipment[19] [20] [21].

1.2 Motivation

There are two methods for a surface texture detection typically, that are touch and sliding[22]. A rough surface can be sensed when a finger was pressed by a sand paper. If a finger pressed a paper, we can detect a flat surface, as well. In touch case, morphology of the surface is sensed through the magnitude of a pressure, pressure distributions, contact areas and etc. For example, in a grating structure, a finger can detect ridge and furrow of the surface texture so that, we can feel that it is uneven surface. Thus, human can perceive surface characteristics by detecting changes of those parameters. However, the touch method has limitations such as resolution and surface shape detection problems.

Another method for surface texture sensing is sliding[23]. Normally, human can feel surface characteristics by sliding more easily than touch. Because many parameters such as vibration, friction, roughness and strains are changed continuously during sliding and then the changing parameters are sensed consistently by tactile receptors. So, sliding is more effective and sensitive method for surface texture sensing. Sensing technologies measuring surface texture have many issues, because various parameter should be considered as well as, the parameters have a unique physical characteristic. In robotic field, a robot finger integrated various sensors has been developed for sensing pressure, temperature, vibration and roughness simultaneously[24], but the robot finger should need complex technologies and has cross-talk problem due to unwanted external stimuli. The thesis was focused on an array sensor which can detect surface textures by sliding mechanism.

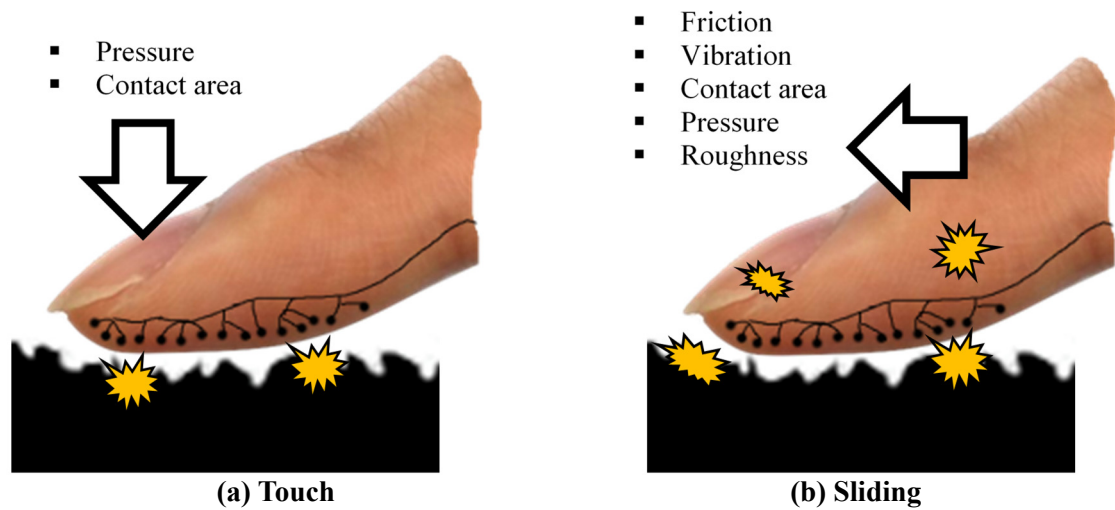


Fig 1.2.1 Images of touch and sliding sensing method. The human can feel a surface texture by both touch and sliding methods. It is generally easy to sense the surface texture under sliding method, because more many parameters are changed and detected by tactile receptors during sliding

1.3 Thesis Overview

The thesis demonstrates an array sensor for surface texture detection and consists of backgrounds, experimental details, results and discussion and conclusion. The human tactile system and previous works regarding to a texture sensing are introduced in Chapter 2. A concept of the sensor array is introduced and additional idea about the array sensor are motivated from the Chapter 2 as well. After that, fabrication, structure and experimental setup are presented in Chapter 3. In Chapter4, sensing results about pressure and sliding, velocity calculation, texture restoration and signal processing are introduced. Lastly, the thesis conclusion and the development possibility and implication of the sensor array for both psychological and physical sensors in the future are presented in Chapter 5.

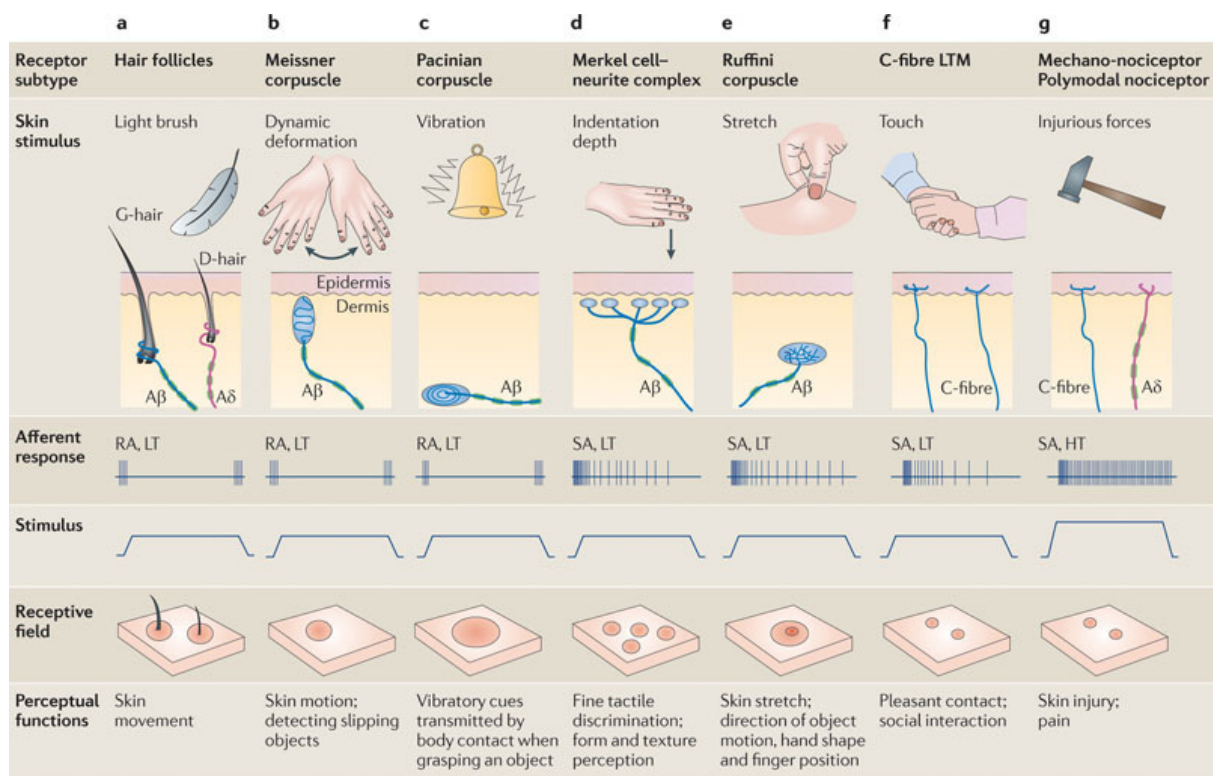
II. BACKGROUNDS

2.1 Human Tactile System

To develop a tactile sensor, it is important to understand and investigate the human tactile system first. Also, understanding the human tactile system is helpful and bring up new ideas about the sensor concept. In Chapter 2, the human tactile system and previous works regarding to a texture sensing are presented.

2.1.1 Tactile Receptors

Tactile receptors are part of the human somatosensory system and also called sensory receptors as well. The tactile receptors make electrical signals when external stimuli were applied and then the electrical signals were sent to the brain though nervous system. So, the tactile receptors act as a transducer [57]. The receptors are located in the end of the peripheral nerve system and respond to specific stimuli such as physical, thermal and chemical stimuli. The tactile receptors are subdividing into mechanoreceptors for pressure and vibration, thermoreceptors for temperature and nociceptors for pain and damage [25]. Especially, mechanoreceptors that responds to pressure or distortion are intimately related with surface texture sensing because the surface texture is a physical stimulation. There are four main mechanoreceptors such as Pacinian corpuscles, Meissner's corpuscles, Merkel's discs, and Ruffini endings and each receptor responds to different physical stimuli [56]. Due to the physical stimuli, the receptor's shapes are deformed and as a result, the action potential was generated.



Nature Reviews | Neuroscience

Fig 2.1.1.1. Characteristics and stimulus responses of mechanoreceptors. [26] Pacinian corpuscles, Meissner's corpuscles, Merkel's discs, and Ruffini endings are typical mechanoreceptors. Each mechanoreceptor has unique characteristics and respond to specific stimuli due to its unique performances.

Pacinian corpuscles determine total amount of pressure and distinguish rough and soft materials. Pacinian reacts in quick action potentials to sudden stimuli, especially to vibrations around 250 Hz so that, they are the most sensitive to vibrations.

Meissner's corpuscles react to moderate vibration (10–50 Hz) and light touch. They are primarily located in fingertips and lips due to their reactivity. They respond in quick action potentials and are responsible for the ability to feel gentle stimuli.

Merkel nerve endings react to low vibrations (5–15 Hz) and deep static touch such as shapes and edges. Due to a small receptive field, they are used in areas like fingertips the most and respond to pressures over long periods.

Ruffini corpuscles respond to sustained skin stretch. They are responsible for the feeling of object slippage and play a major role in the kinesthetic sense and control of finger position and movement.

2.1.2 Nervous System of Touch

In case of contact with a certain object, tactile receptors detect surface information of the object through the deformation of mechanoreceptors. Each mechanoreceptor measures a small portion of the surface texture and encodes the tactile information as a train of action potentials. This encoding process is similar to digitizing and coding analog signals by an analog-to-digital (A/D) convertor [27]. The action potential is transmitted to the central nervous system(CNS) for higher level processing and interpretation via multiple nerves up to the spinal cord and via two major pathways: spinothalamic and dorsal-column-medial-lemniscal (DCML). The DCML quickly conveys information related with pressure and vibration to the brain and helps in spatial and temporal comparisons of the stimuli [25].

The Dorsal Column-Medial Lemniscal Pathway From Tactile receptors to the Brain

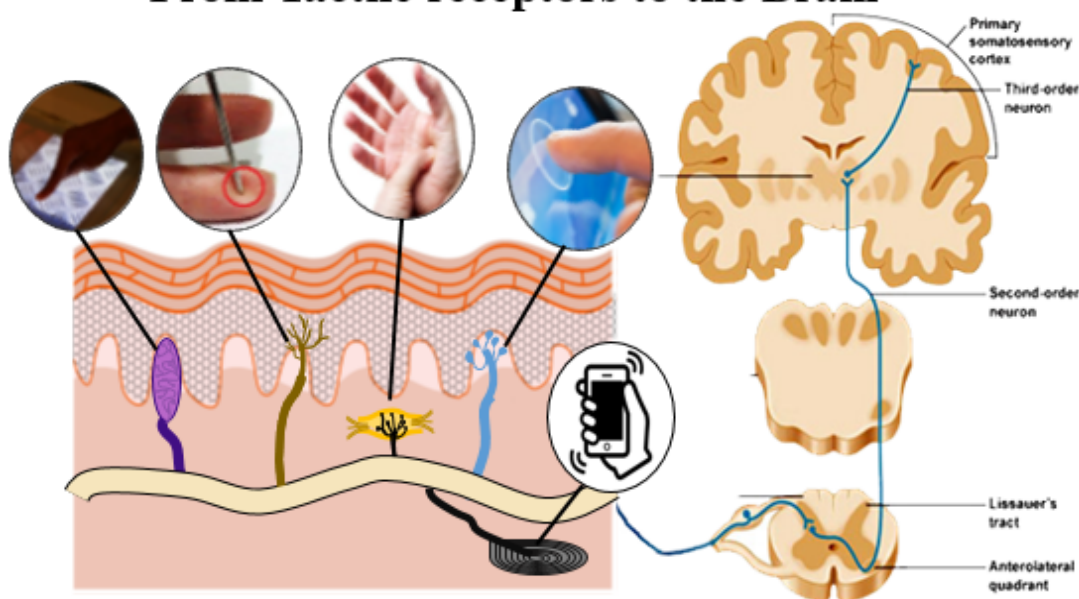


Fig 2.1.2.1 The dorsal column-medial lemniscal pathway.

2.2 Surface Textures

A surface texture is one of the important factors related with friction, adhesion, transfer and surface properties. Especially, surface information such as friction, roughness and vibration are related with the surface texture [59]. So, researches about surface textures have been studied for a long time in various fields. Surface texture is typically defined by texture shape, texture's pattern, roughness and etc. To measure the surface characteristics, various measurement technologies have been developed. AFM(Atomic Force Microscope) is a kind of technology scanning surface texture. Small tip contacts with a surface during scanning on the x-axis and height of the tip is changed due to the surface texture such as pattern and shape at the same time. Laser beam detects a small amount of tip's height changes and indicates surface information containing both x and z-axis images.

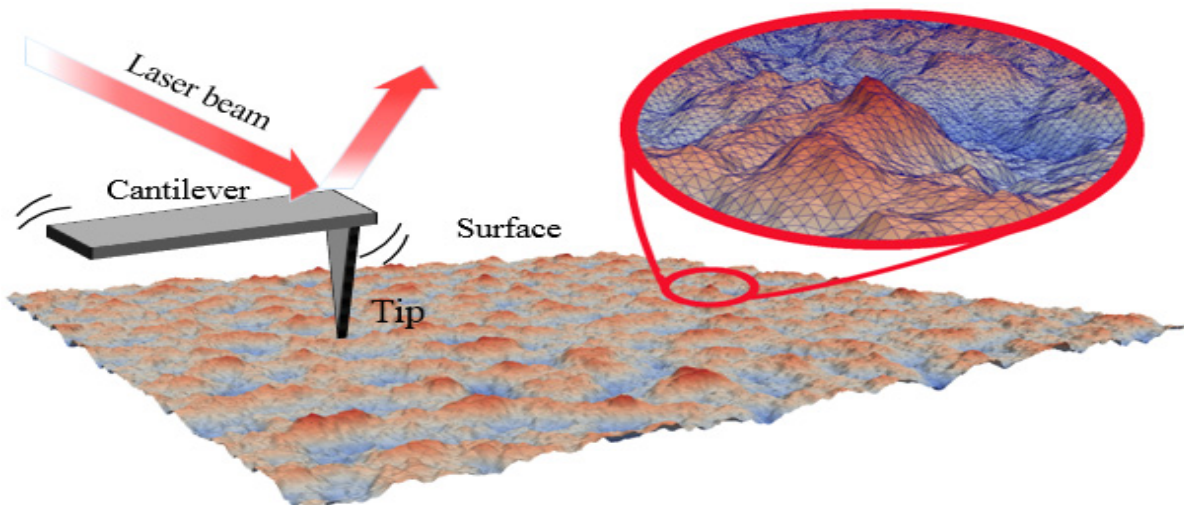


Fig 2.2.1 AFM mechanism and scanning image

The AFM can get a 3D image of surface and also measure several surface information. The mechanism of the AFM is very useful for surface sensing. The advantages of AFM arise from not only scanning method but also tip's height changes. Basically the tip is moved on x and y-axis by an actuator during scanning a surface. Simultaneously the tip also gets z-axis information of the surface's ridge and furrow through contacting with the surface. Thanks to the mechanism, x and y-axis information can be collected by scanning method and z-axis

information can be measured by tip's position changes. Thus surface features such as texture's shape, pattern and relief can be measured by analyzing the position changes.

2.3 Previous Works for Sensing Surface Textures

Humans are very proficient in recognizing surface properties based on the sense of touch, but there are many issues how a robot can recognize the surface properties [28]. Studies related with perceiving and recognizing surface textures also have been developed to mimic the human tactile receptors in haptic and robotic field. As well as, many engineering researches have been conducted to measure the surface properties through the robotic finger. Some robotic researches have been approaching to collect surface properties such as friction, vibration, roughness etc. by sliding or gripping mechanism. In the robotic field, because gripping and slip prevention are important issues, robotic fingers applied feedback loop or complex algorithm have been developed to perceive surface textures[29] [30] [31]. However, it is hard to find studies about tactile sensors which detect surface textures relatively. Only some optical and piezophotonic sensors were proposed as a surface detection sensor [19].

2.3.1 Friction

Friction measurement is one of the widely used method to measure surface textures because it has intimately relationship with surface texture. Various researches concerning friction and friction coefficient have been proposed to measure surface texture. Normally, friction was measured by a friction measurement system through a sliding experiment and then the measured friction values was classified according to surface properties

such as shape, pitch etc. Kawasegi et al. demonstrated that fluctuation of the friction coefficients was related to the sticky and uneven sensations. They were emphasized that the magnitude of the coefficient of friction, surface roughness and deflection were not strongly affected by the texture, as well as, the texture pitch was the most significant factor determining the surface pattern and tactile sensory [32]. Xiaojing et al. proposed a new surface classification based on the frictional properties of the surfaces by using the quasi-static LuGre model and Newton-Raphson method. The experiment results showed a high accuracy in surface classification [33]. Gee et al. [34] developed a friction device for measuring dynamic friction coefficients between finger and surface of various materials such as rubber, steel and glass in order to accurately mimic sensory perception.

2.3.2 Roughness

Because roughness is one of the important parameters determining surface properties, roughness detection technologies such as contact stylus type, optical probing type and interferometer type have been developed so far. The stylus type method analyses roughness information by scanning the material surface in a contact measurement but it can be damaged from the surface or damage to the surface. Another method is non-contact measurement; this method obtains roughness information by analyzing the reflected light source from material surface. Yang et al. [35] proposed a method of roughness estimation with Mueller matrix. Much information of roughness can be contained in elements of the Mueller matrix, so that experimental results showed efficiency of roughness detection and precision improvement. Nemoto et al. [36] developed a roughness measurement standard with irregular surface topography for improving 3D surface texture measurement. They got roughness data by using the 2D A-R model and then restored a 3D surface roughness based on the measured data.

2.3.3 Vibration

Measuring vibration for surface texture detection is also widely used in sliding mechanism as like friction measurement. Humans can easily feel a vibration through the Pacinian corpuscles which is one of the mechanoreceptors, so many vibration sensors mimicking the receptor's vibration detecting mechanism have been introduced [37]. Jamali et al. [38] classified surface textures based on the frequencies and amplitudes of the vibrations occurred from the sliding contact. They developed an artificial finger embedded strain gauges and PVDFs and then slid the finger with various surfaces. Embedded PVDF sensors generated frequency responses according to the surface texture and then an applied algorithm calculated the frequency results to classify different textures. A nanogenerator type tactile sensor translating texture information into sequence of electric pulses was proposed in [39]. The texture information is conveyed by the amplitude of current and frequency of the electric pulses. Unlike previous sensors, this NG tactile sensor can not only indicate a fine texture but also figured out an acceleration of sliding motion by using a simple analyze due to its piezoelectric property [40].

2.3.4 Optical Sensor

Tactile sensors based on optical equipment detect a surface texture from changes of the light intensity [41]. There are three types optical sensor; opto-mechanical, fiber-optic, internal reflection. Those kinds of sensors have good sensitivity and reactivity in case of the slip detection especially, but additional equipment such as light source, light guide, photo-detector etc. should need to measure the changes of the light intensity. Tanie et al. proposed optical sensor based on frustrated internal reflection. When the sensor contact with certain surface, light loss arises at the contact point because of scattering. As a result, internal light

intensity was frustrated and shadow appeared at the contact area. In opto-mechanical type, optical shutter is acted to modulate light transmission between a light emitting diode and a photo-detector depending on applied external pressure.

2.3.5 Piezophotonic Sensor

Piezophotonicity is the ability to convert a pressure into a light. Maheshwari et al. [19] demonstrated a thin film device to sense texture by touch. The sensor showed a pattern of surface texture or contact area by emitting light. The light intensity increased proportional to applied normal pressure. A nanowire based sensor array imaging of pressure distribution was proposed in Pan et al [42]. Zinc oxide nanowire was used as light emitting diode and the sensor has high resolution due to high density of ZnO nanowires. Those piezophotonic sensors also have a self-biasing characteristic.

III. EXPERIMENTAL DETAILS

3.1 Piezo Sensor Array

In the thesis, a tactile sensor used piezoelectric material and array structure was introduced for surface texture sensing. Because the piezo sensor array has a similarity with the human tactile receptors. Also, flexible substrate and soft materials were used to the array sensor to imitate human skin.

Sensors applied piezoelectric materials have been developed in various fields. Jang et al. [6] demonstrated a piezoelectric sensor for pressure detection and Chun et al [43] introduced a tactile sensor that can detect surface texture and sliding information. There are various types of piezoelectric materials such as ceramic, crystals and polymer, so that it is possible to use various fabrication processes and obtain a variety of piezoelectric properties depending on the materials. In addition, the ability of piezoelectricity is very similar with tactile receptors which translate external stimuli into electrical signals. The electrical signals arise from piezoelectric materials have high sensitivity and fast response characteristics, so that piezoelectric sensor is more suitable for a dynamic movement detection than static movement [44]. PVDF-TrFE(poly[(vinylidene fluoride-co-trifluoroethylene)]) which is one of the popular piezoelectric copolymers was used for the piezo sensor array suggested in this paper. The material has high sensitivity due to its high piezoelectric coefficient and fast response time. Also, the copolymer allowed easy-fabrication process and flexibility characteristics, as well [45]. A PZT (lead zirconate titanate) ceramic which has very high piezoelectric coefficient is now used to tactile sensors to have very high sensitivity. However, those sensors applied the PZT have complex fabrication process and non-flexibility problem, because PZT is ceramic [45]. Thus, it is

important to use appropriate piezoelectric materials depending on purpose of sensors, structure of the sensor, and fabrication process.

A structure of sensor is also important factor to determine a sensing ability. Many research groups have introduced a variety of sensor structures so far. A pressure sensor having double ZnO nanowire layers was introduced to enhance the sensor performance [46]. Thanh-Vinh [9] et al. proposed a piezo-resistive sensor for pressure and shear force sensing. It consists of piezoresistive cantilevers and PDMS cap. The PDMS cap induces deformation of cantilevers when external strain was applied and then resistance of cantilevers was changed as a result of its deformation. A flexible sensor having TFT array was proposed for simultaneous sensing of pressure and temperature [12]. A tactile sensor array applied PDMS bump layer was introduced for three-axis force and slip detection as well [5]. The piezo sensor array introduced in the thesis also has an array structure for detecting surface textures and the array structure allowed that the sensor is able to have high resolution and pressure distribution detection.

3.1.1 Principles of Piezoelectricity

Piezoelectricity is linear interaction between mechanical and electrical systems in non-centric crystals or asymmetry structure materials [45]. This phenomenon produces the electric charge accumulation in certain materials in response to applied mechanical stress [59]. It is commonly defined as the direct piezoelectric effect which generates the electric polarization proportional to the external stress. The stress leads to dielectric displacement and the displaced dielectric manifests an internal electric polarization [47]. The converse piezoelectric effect is a phenomenon that the internal stress appears, when an external electric field is applied. It should be noted that the piezoelectric effect depends on the asymmetry of the crystal.

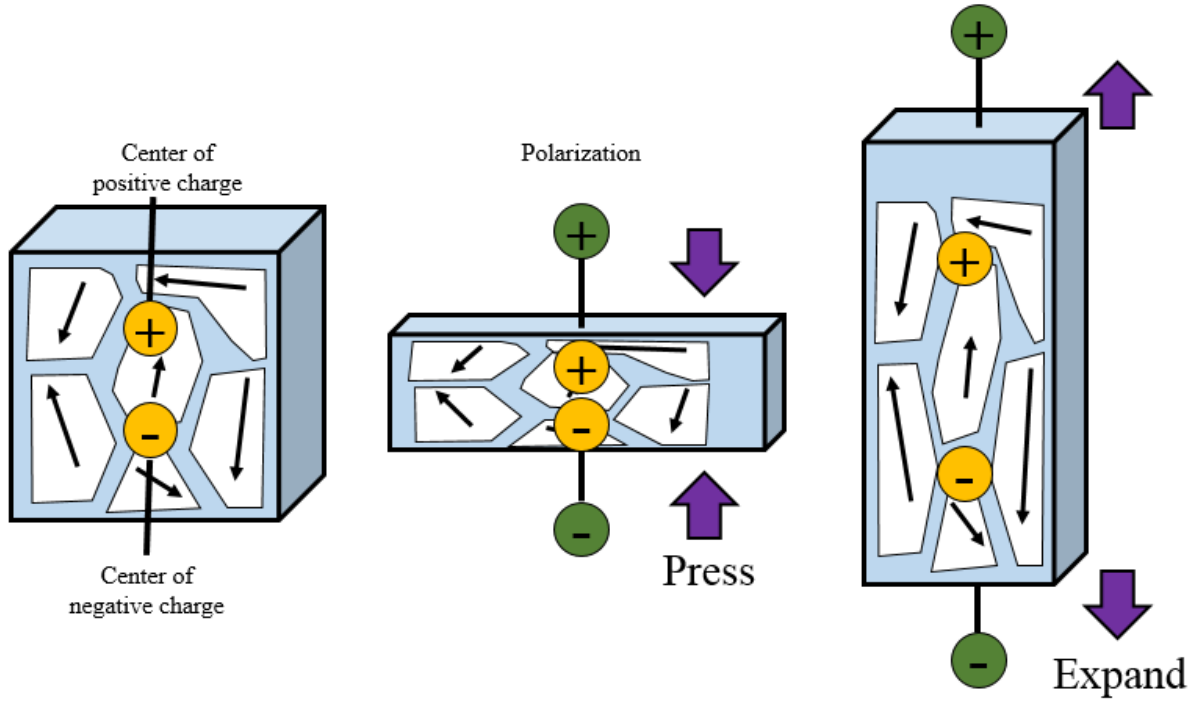


Fig 3.1.1.1 The piezoelectric effect mechanism.

A material having central symmetry is hard to have piezoelectricity. So, mechanical and electrical properties of the piezoelectric materials are coupled with linear relationship between applied stress and internal electric polarization. The resulting charge density D_i induced by the applied stress is defined as [47]

$$D_i = d_{im}\sigma_m \quad (3.1)$$

where d_{im} is a direct piezoelectric coefficients and σ_m is the components of the stress tensor. Conversely, the other abilities of piezoelectric materials consist to contract or expand when an external electric field is applied. This strain is described as follow

$$x_m = d_{km}E_k \quad (3.2)$$

where d_{km} is an inverse piezoelectric coefficients and E_k is the components of the electric field.

To fully understand the piezoelectric material coefficients, following equations derived from the coupling of elastic and dielectric properties is necessary

$$D_i = \varepsilon_{ik}E_k + d_{im}\sigma_m \quad (3.3)$$

$$x_n = d_{kn}E_k + s_{nm}\sigma_m \quad (3.4)$$

$$E_k = \beta_{ik}D_i - g_{km}\sigma_m \quad (3.5)$$

$$x_n = g_{in}D_i + s_{nm}\sigma_m \quad (3.6)$$

$$D_i = \epsilon_{ik}E_k + e_{in}x_n \quad (3.7)$$

$$\sigma_m = -e_{km}E_k + c_{nm}x_n \quad (3.8)$$

$$E_k = \beta_{ik}D_i + h_{km}x_n \quad (3.9)$$

$$\sigma_m = -h_{im}D_i + c_{nm}x_n \quad (3.10)$$

where c_{nm} and s_{nm} are elastic stiffness and elastic compliance tensor, ϵ_{ik} is the dielectric permittivity, β_{ik} is the dielectric impermeability and d_{im} , g_{im} , h_{im} , e_{im} are piezoelectric coefficients. Equations of state (3.3), (3.4), (3.5) and (3.6), belong to the description of direct piezoelectric effect. On the other hand, equations of state (3.7), (3.8), (3.9) and (3.10), belong to the description of inverse piezoelectric effect [47].

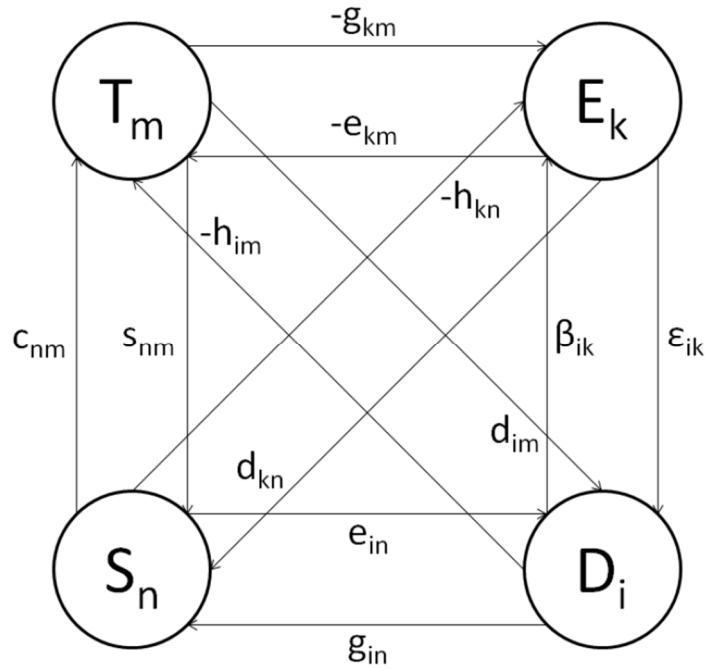


Fig 3.1.1.2 Relations among electrical and mechanical quantities [47].

Piezoelectric effect is described by four different material coefficients according to the choice of independent variables. Relationship of piezoelectric materials coefficients between mechanical and electrical quantities were represented in the Fig 3.1.1.2. Arrows pointing from mechanical to electrical quantity represent direct piezoelectric effect. On the contrary, arrows pointing from electrical to mechanical quantity represent the inverse piezoelectric effect.

In the paper, basic piezoelectric property which transfer pressure into the voltage was used as the main mechanism of the piezo sensor array.

3.1.2 Piezoelectric Materials

Nowadays a variety of piezoelectric materials such as crystals, ceramics, polymers and composites are applied in the sensor field [48].

Quartz, lithium niobate(LiNbO_3) and lithium tantalate(LiTaO_3) are the typical piezoelectric crystals. The piezoelectric crystals are used in various field, and also utilized as oscillators and surface acoustic devices. Quartz is also the most popular single crystal piezoelectric material and it is used for low loss transducers because of its high mechanical quality factor. Lithium niobate(LiNbO_3) and lithium tantalate(LiTaO_3) have high electromechanical coupling coefficients for surface acoustic wave as well, so that those materials are used for SAW devices [45].

Barium titanate(BaTiO_3) and PZT are most popular piezoelectric ceramics. Especially, PZT ceramics have been widely used in a variety of applications for a long time. The PZT has excellent piezoelectric properties that can be designed to meet specific purposes by doping and also has high electromechanical coupling coefficients(k) and piezoelectric coefficient(d). Thus PZT ceramics are suitable for high power transducers and sensor [48].

Piezo-composites comprising piezoelectric ceramic and polymer phases are promising materials because of their excellent properties. The advantages of the composites are high coupling factors, low acoustic impedance, good matching to human tissue, mechanical flexibility and broad bandwidth property. So, the piezoelectric composite materials are especially useful for underwater sonar and medical diagnostic, ultrasonic transducer applications [48].

Piezoelectric polymers have a lower piezoelectric coefficient compared with the piezoelectric ceramics. However, the low value of permittivity of the polymers leads to high values of voltage constant. Also they have advantages such as flexibility, low density, lightweight and low cost as well. PVDF (polyvinylidene difluoride) was first discovered as piezoelectric polymer by Kawai [47]. Although the PVDF has different mechanism of amorphous and semicrystalline piezoelectric materials, it can also have piezoelectricity. Because the PVDF has certain alignment of molecules, the alignment has an ability to make internal polarization when stress is applied. The molecular structure of PVDF is simple; the monomer consists of two vinyl atoms of carbon with one of them bringing two fluorine atoms. The PVDF has different phases depending on the reciprocal orientation of the C-F₂ dipoles and the phases have different piezoelectric properties. The most important phase is β -PVDF phase, because it shows ferroelectric behavior. In this phase, the dipoles CF₂ are all oriented in the same direction. Recently, PVDF polymer is used with copolymers to enhance the piezoelectric properties. The addition enhancement procedure increase a β -phase crystallinity of the polymer up to 90% so, PVDF-TrFE (polyvinylidene difluoride trifluoroethylene) has much stronger piezoelectric property than a normal PVDF [47].

The PVDF-TrFE copolymer was also applied to the piezo sensor array introduced in the thesis due to its flexibility, high sensitivity, easy-fabrication process and capacity of dynamic movement sensing.

3.1.3 Array Structure

Array structure consists of a systematic arrangement of similar pattern in rows and columns [60]. Many kinds of sensors are applied to the array structure to have a variety of advantages such as high resolution, slip detection and ability of pressure distribution sensing [49]. The array structure was also applied to the piezo sensor array, because many cells constituting the array structure plays a role in the human receptors. The human receptors are very densely placed in human skin. If the receptors are not distributed densely, it is hard to feel external stimuli well. Thus, a sensor having a high resolution is essential to mimic the human touch system, so that an array structure is the best candidate to achieve the high resolution characteristic. However, the array structure also has problems concerning with too many electrodes, cross-talk, size effect and etc. Matrix structure was proposed to reduce the many electrode problems but, cross-talk and confusion under multi-touch condition also are occurred as well [50] [51].

3.1.4 Soft Material

The human can feel surface textures through a deformed skin. For example, the amount of a skin deformation is different depending on an applied pressure so, human can distinguish between spike shape and dome shape due to the pressure difference. Thus, we thought that mimicking the human skin should be a key to sense surface textures. A soft material was particularly applied to the bottom of the sensor to induce a sensor deformation to mimic the human skin. We applied soft materials such as sponge and PMDS to the sensor and then optimized. Some papers demonstrated sensors embedded in soft material like PDMS to sense shear force [52] [53]. However, it was rare to apply a sponge to the sensor so, it was a unique characteristic of the piezo sensor array introduced in the thesis.

3.2 Fabrication and Structure of Piezo Sensor Array

The piezo sensor array consists of bottom layer for a common electrode and top layer for an array structure. Fig 3.2.1 shows a fabrication process of the top layer. First, a polyimide film was cleaned by acetone and IPA to remove organic residues and particles by using ultrasonic cleaner. The polyimide film substrate was taped on a glass to fix the film during spin coating process. Then, negative photoresist (AZ nLOF-2035) was spin-coated with 3000 rpm. The thickness of the photoresist depends on the revolution per minute(rpm) of the spin-speed. In the case, the negative photoresist had the 3 μm thick under 3000 rpm condition. The reason negative photoresist was chosen is that it can make a clean sidewall pattern than positive photoresist after UV-expose and lift-off process. After coating the photoresist, the coated polyimide substrate was put in a hot-plate at 130°C for 1 minutes to bake the negative photoresist. After baking, the photoresist was exposed by ultraviolet (UV) ray to form an array pattern. After UV expose process, exposed photoresistive was baked again at 130°C for a minutes and a half. The process is called as hard baking. Hard-baked samples were dipping in AZ-300 developer for 1 minute and 30 seconds to remove photoresist residues and develop the array pattern. Developed samples were rinsed by deionized (DI) water for 1 minute and dried by blowing N₂ gas. After photolithography process, 50 nm thick Chrome (Cr) and the 100 nm thick Au were deposited by using a radio frequency (RF) magnetron sputtering system at an input power of 200 W to make a metal layer of the array patten. The Cr layer was added to enhance the adhesion between the polyimide substrate and the Au layer. After Cr/Au electrodes were deposited, the electrode array patterns were obtained through the lift-off process, which photoresist residues were removed by dipping in acetone and rinsing in isopropyl alcohol (IPA). The array patterns consist of 36 cells and each cell has 1mm² size with 2mm pitch. The PVDF-TrFE 15% solution was made by mixing PVDF power with 2-butanone solution. The mixed solution was stirred to solve the PVDF power entirely. Then the PVDF-TrFE solution

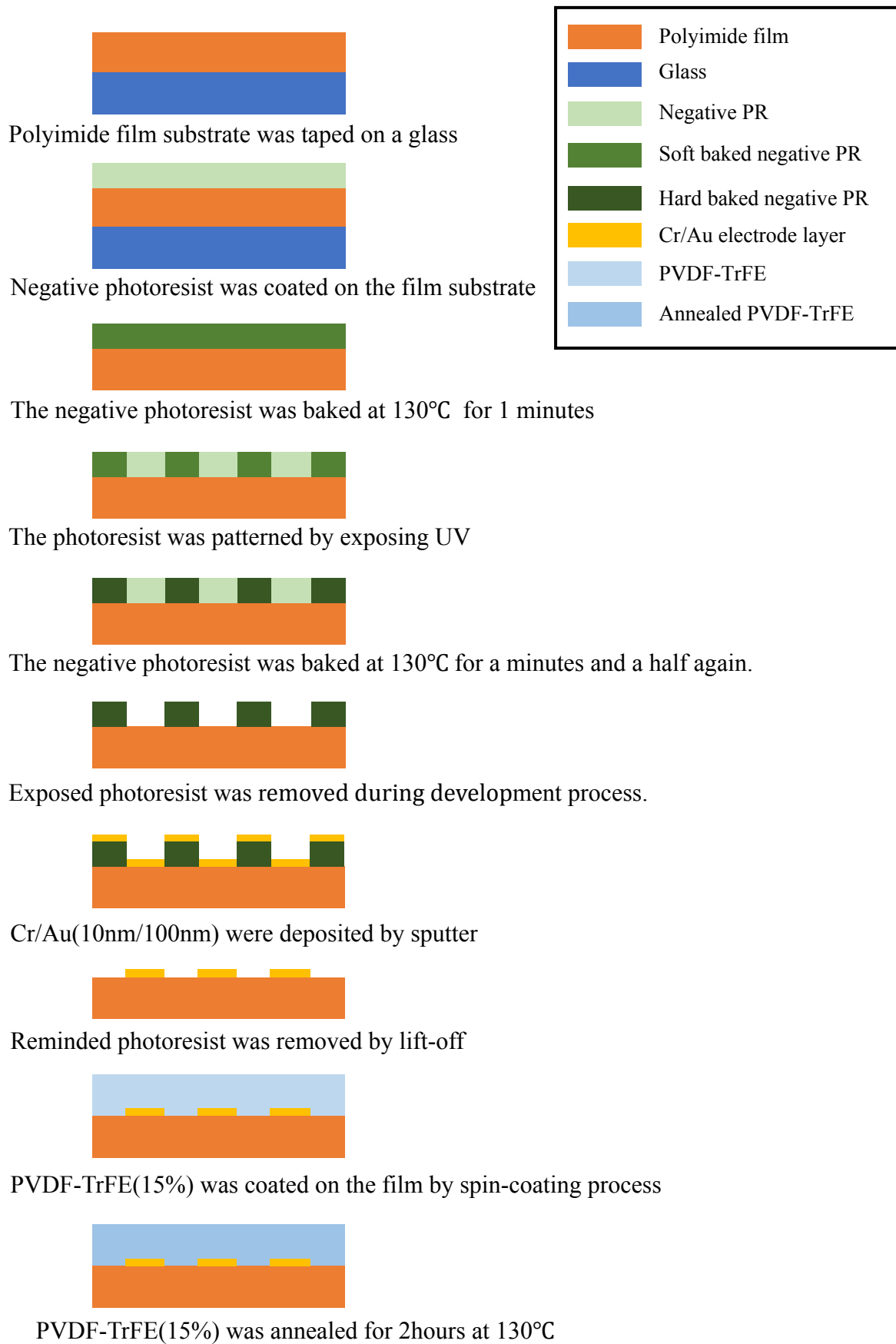


Fig 3.2.1 Schematic of the top layer fabrication process of piezo sensor array

was coated with 3000rpm upon the array patterns. After PVDF-TrFE was coated on the film substrate, the sample was annealed at 130°C for 2hours. On the other hand, bottom layer fabrication process is much easier than the top layer case. Because the bottom layer was used as a common electrode, Cr/Au layers (100 nm thick Cr and the 100 nm thick Au) were deposited on all over a polyimide substrate (Fig3.2.2).

To set-up the piezo sensor array, the bottom layer was placed on a floor first and then the top layer was overturned to make PVDF-TrFE layer meet the electrode layer of the bottom layer. After that, both layers were taped to fix them (Fig.3.2.3).



1. Polyimide film was cleaned by acetone and IPA



2. Cr/Au(10nm/100nm) were deposited by sputtering system

Fig 3.2.2 Schematic of the bottom layer fabrication process of piezo sensor array

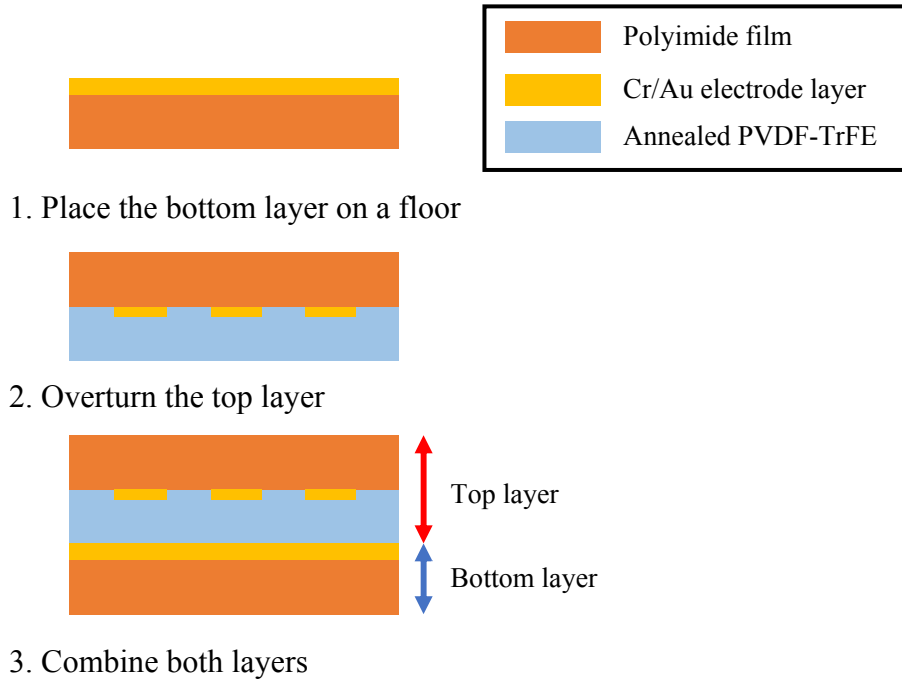


Fig 3.2.3 Schematic of the piezo sensor array set-up

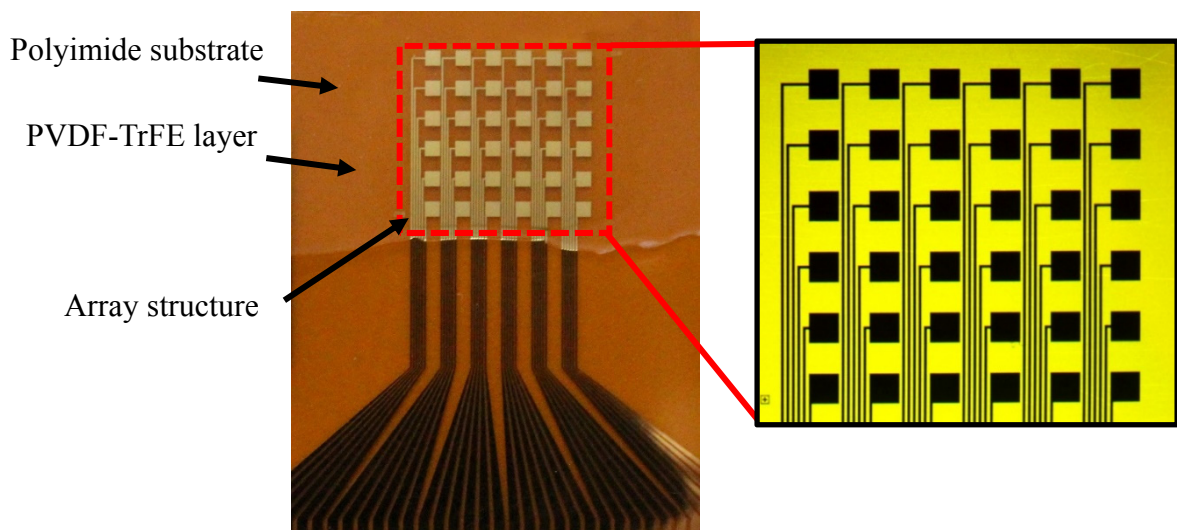


Fig 3.2.4 Optical images of the top layer of piezo sensor array

3.3 Design of Textures

In the paper, three different textures were 3D modeled and used for surface texture sensing. The textures having bump, spike and dome shapes were fabricated by a 3D printer. The textures had successive patterns having bump, spike and dome shapes with 3mm pitch in common. The bump texture had a 1mm width and intervals of the bump patterns was 2mm. In the spike case, spike shape had around 0.15mm width because of a resolution limit of the 3D printer. All textures are designed as a detachable form for various texture sensing experiments.

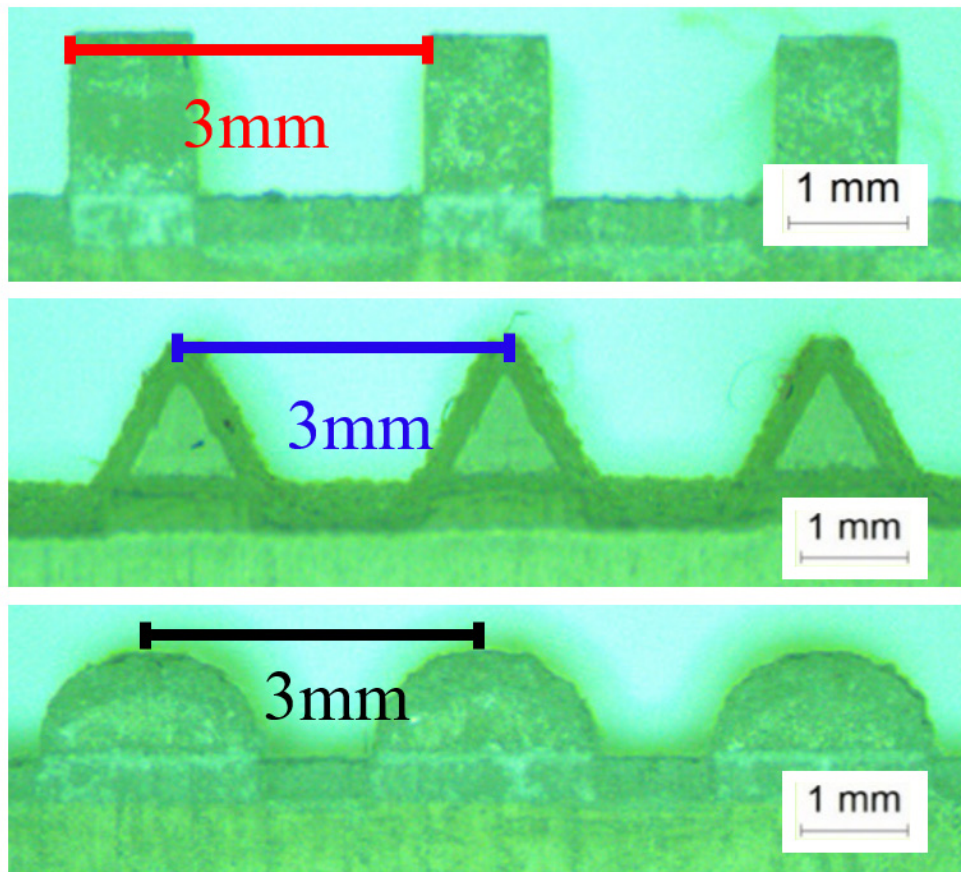


Fig 3.3.1 Enlarged textures designs of the bump, spike and dome shapes. All textures had 3mm pitch.



Fig 3.3.2 Optical image of the three different textures. The textures were designed to be removable and the textures were mounted on a linear stage for sliding experiments

3.4 Experimental Setup

In section 1.2, touch and sliding methods were mentioned for a surface texture sensing. In the paper, basically touch experiment and sliding experiment were proceeded respectively to compare which method is more suitable for texture detection. A 200g weight was used to the touch and sliding experiment for same experimental condition. The piezo sensor array was pressed by the different textures in the touch experiment. An occurred piezoelectric signals were analyzed, whether the result signals have texture information or not. In the sliding experiment, a linear stage (X-LHM100A, Zaber) was used to slide the three textures. The linear stage controls such as sliding velocity, move distance, acceleration could be set through a Zaber software. The texture stage was mounted on the weight container and each texture was mounted on the texture stage. In sliding experiment, sliding velocity was set to 30mm/s as uniform velocity normally. Besides, the sliding experiment was proceeded twice under soft material and non-soft material condition. To measure the electrical signals of the piezo sensor array, mixed signal oscilloscope (MSO-X 2024A) was used.

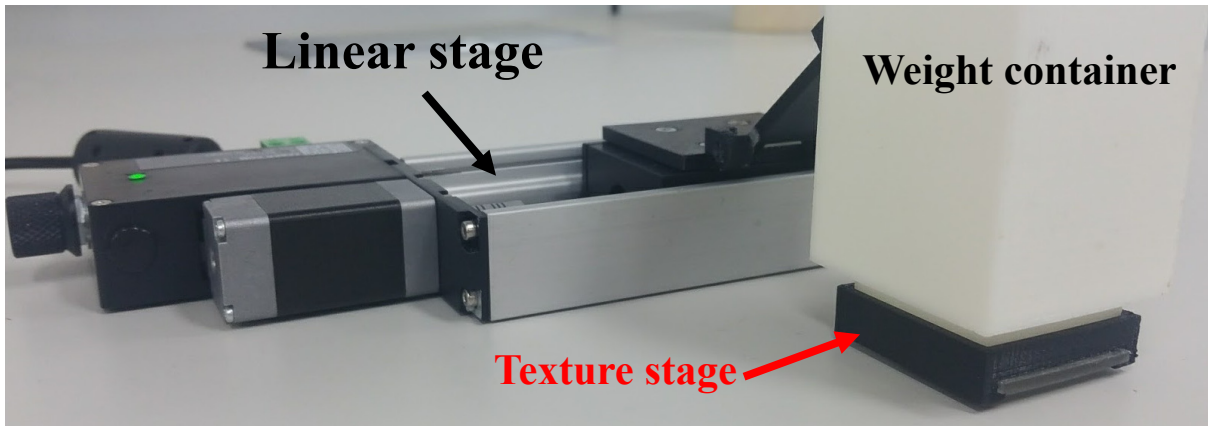


Fig 3.4.1 Experimental set-up image of linear stage with weight container and texture stage.

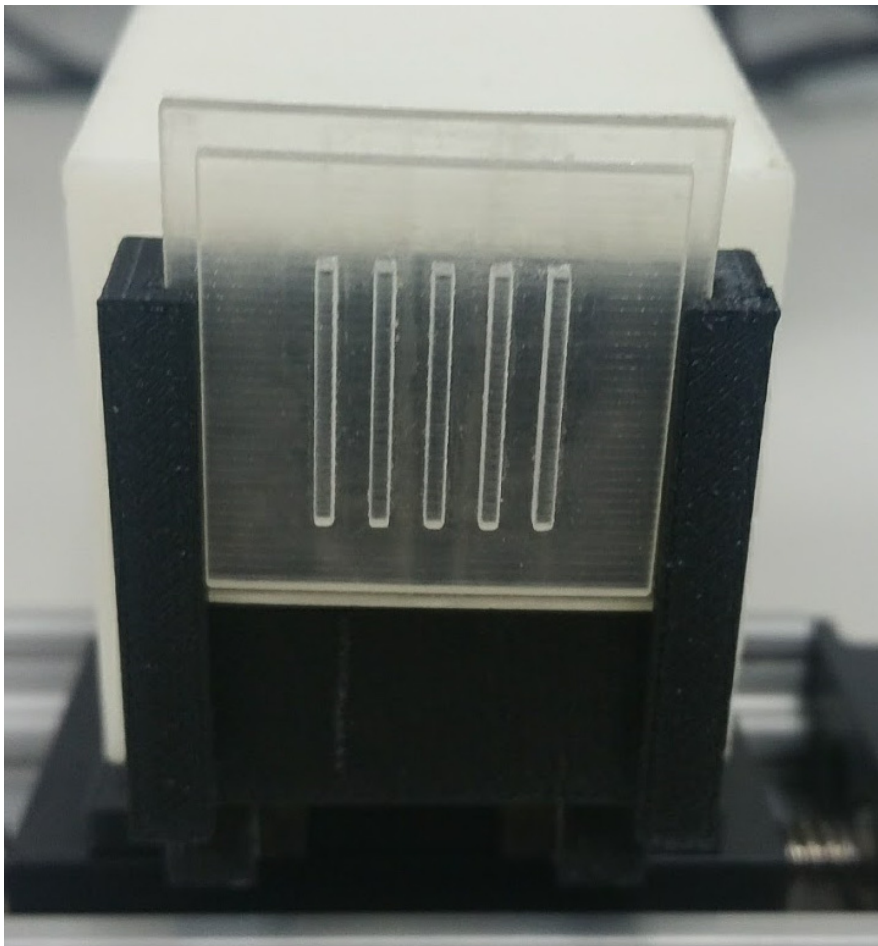


Fig 3.4.2 Mounted the bump texture to the texture stage.

IV. RESULTS AND DISCUSSION

4.1 Characteristics of Piezo Sensor Array

Touch and sliding experiment were proceeded to measure a characteristic of piezo sensor array in this chapter. We analyzed that result piezoelectric signals arisen from the array sensor. The results of touch and sliding experiments were different and had unique characteristics. The results were similar with an assumption which is a surface texture can be sensed more easily under sliding condition than touch case. Also, the piezo sensor array had a high resolution characteristic as expected due to its array structure.

4.1.1 Touch Experiment

We checked that the sensor array can measure a pressure basically. The sensor array was pressed by the three different textures having bump, spike, and dome shapes. A 200g weight was used for the same experiment conditions. An occurred voltage was expressed by the color mapping in Fig 4.1.1.1 b.c.d. In spite of same 200g weight condition, applied pressures were different depending on shapes of texture. A 0.4V was occurred in the bump texture due to its large contact area (Fig 4.1.1.1.b). On the other hand, a 0.6V was occurred under the spike texture, because a normal pressure was strongly applied (Fig 4.1.1.1.c). We confirmed that there were only voltage changes depending on texture shapes in the touch experiment. From this results, the sensor could not detect all textures position and distinguish texture shapes due to its resolution limit. It should be a big problem because if the sensor was pressed strongly by the bump texture, the sensor cannot distinguish whether it is bump or spike. Therefore, the array sensor could not perfectly detect surface texture through the touch experiment.

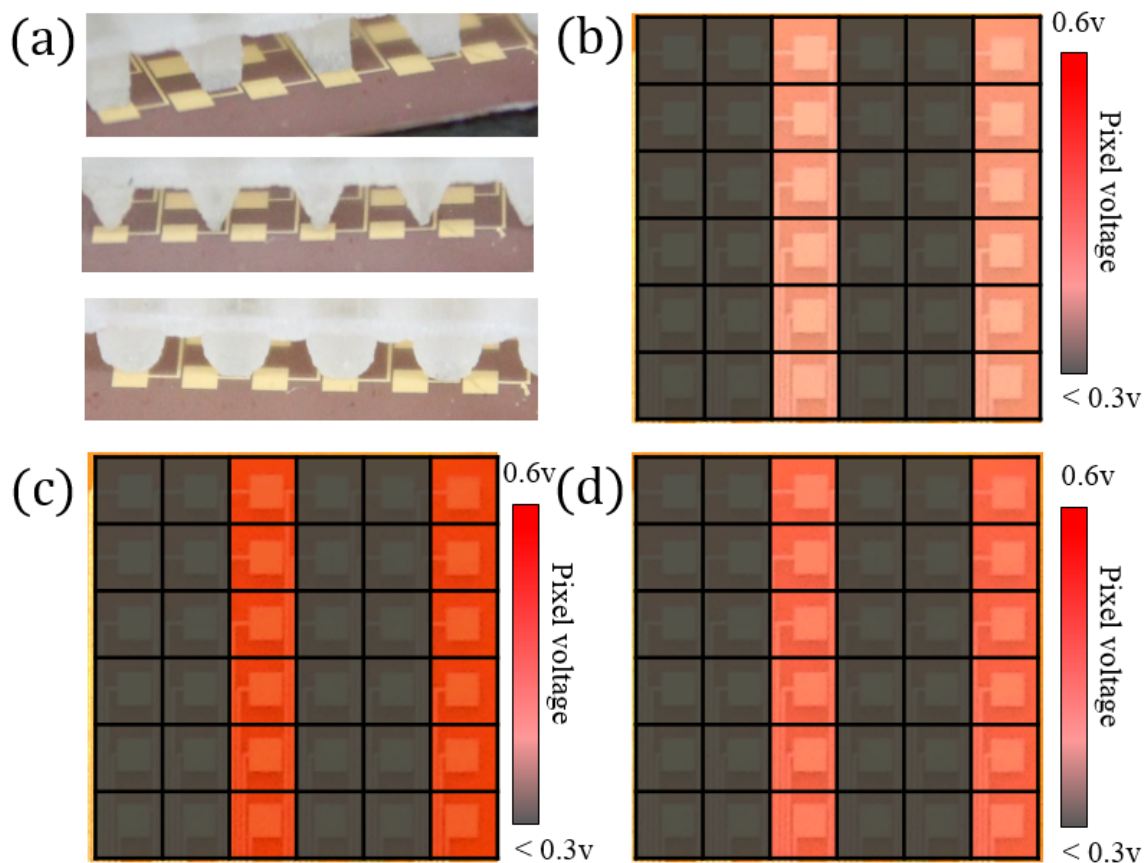


Fig 4.1.1.1 The results of touch experiment with various textures. (a) Images of three different textures with the array sensor. (b),(c),(d) The pressure mapping images of bump, spike and dome textures respectively. The output voltage increased corresponding to the pressure.

4.1.2 Sliding Experiment

Sliding is another method for surface texture detection. Three different textures were slid on the sensor for the sliding experiment. The 200g weight was also used for the same experimental condition. The textures and weight were mounted on a linear stage (X-LHM100A, Zaber) and then moved at 30mm/s. In the experiment, we found that result signals of pressure and sliding experiment were different. A piezoelectric signal induced by pressure had a very high slope and high output voltage normally. However, piezoelectric signals induced by sliding

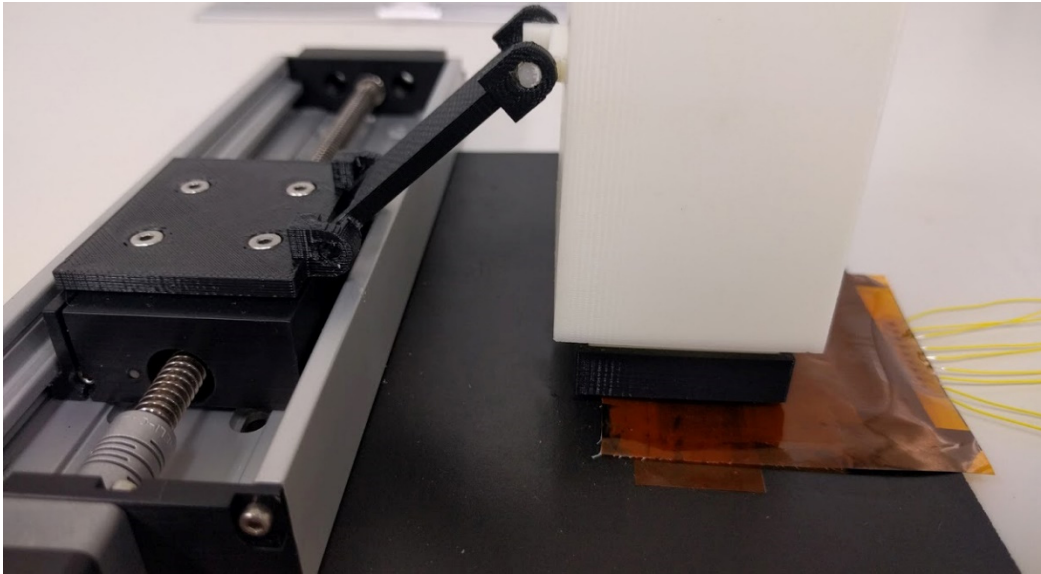


Fig 4.1.2.1. Image of sliding experimental setup with leaner stage (ZABER, X-LHM100A). The block bottom layer is a sponge. Weight is put into the white container and textures were mounted on the block texture stage.

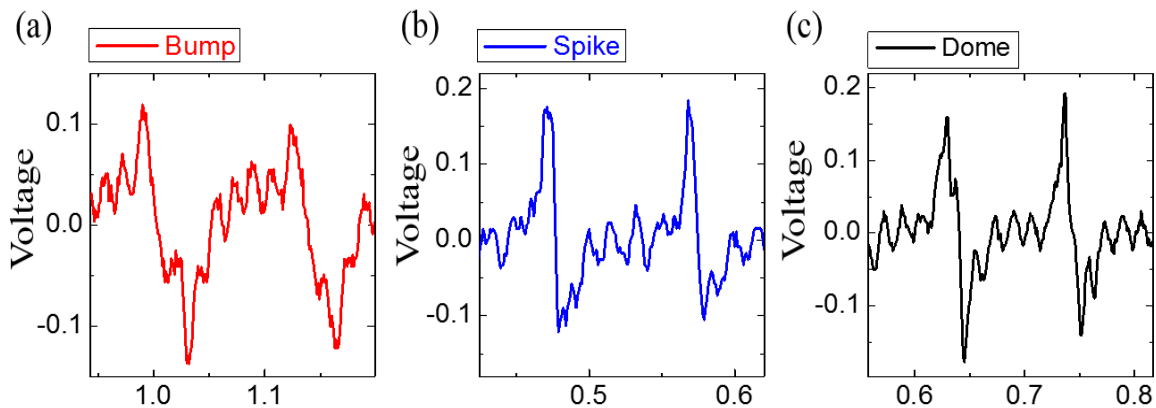


Fig 4.1.2.2. A sliding signals of the different textures from the sensor array. The sliding signal of bump texture shows a low voltage than other texture's signal. Also The signal shape is more broad and slope of signal is gentle than other signals. (b), (c) Both sliding signals shows a similar output voltage, slope and signal shape as well. The bump signal can be distinguished from spike and dome, but there are some problems to distinguish the spike and dome signal.

had a gradual slope and low voltage than the pressure like Fig 4.1.2.2. The lowest voltage appeared in the bump texture and a twice voltage was occurred in spike and dome textures. Apart from the voltage, each sliding signal wave form was a little bit different depending on the textures. A sliding signal of the bump texture was broad and had a gradual slope rather than

other signals (Fig 4.1.2.1.a). On the other hand, the signals of spike and dome textures were narrow and had a sharp slope than bump (Fig 4.1.2.1.b.c). So, it was able to distinguish a bump texture from spike and dome textures by comparing the signal wave forms. However, there was a limitation to distinguish between spike and dome textures because of their similar output voltage and signal wave forms.

We compared the result signals of three different textures by a signal processing called the correlation method. Correlations are useful because they can indicate a statistical relationship between two random variables [54] [61]. A correlation coefficient is a number that quantifies correlation and dependence and meaning statistical relationships between two observed data values.

If two observed data values have N scalar observation, then the correlation coefficient is defined as [54]

$$\rho(A, B) = \frac{1}{N-1} \sum_{i=1}^N \left(\frac{A_i - \mu_A}{\sigma_A} \right) \left(\frac{B_i - \mu_B}{\sigma_B} \right), \quad (1)$$

where μ_A and σ_A are mean and standard deviation of A, respectively, and μ_B and σ_B are also the mean and standard deviation of B. The correlation coefficient can be defined in terms of the covariance of A and B:

$$\rho(A, B) = \frac{cov(A, B)}{\sigma_A \sigma_B}, \quad (2)$$

The correlation coefficient matrix of two data is the matrix of correlation coefficients for each pairwise variable combination,

$$R = \begin{pmatrix} \rho(A, A) & \rho(A, B) \\ \rho(B, A) & \rho(B, B) \end{pmatrix}. \quad (3)$$

Since A and B are directly correlated to themselves, the diagonal entries are just 1, that is,

$$R = \begin{pmatrix} 1 & \rho(A, B) \\ \rho(B, A) & 1 \end{pmatrix} \quad (4)$$

By using the correlation coefficient method, signal relationships between bump, spike and dome($\rho(A,B)$, $\rho(A,C)$, $\rho(B,C)$) were calculated as 0.0413 0.1605 and 0.6661 respectively. The results also proved that sliding signal of bump was different compared with spike and dome signals, as well as sliding signals of spike and dome had similar signal wave form and output voltage. It means that it is hard to distinguish between spike and dome signals.

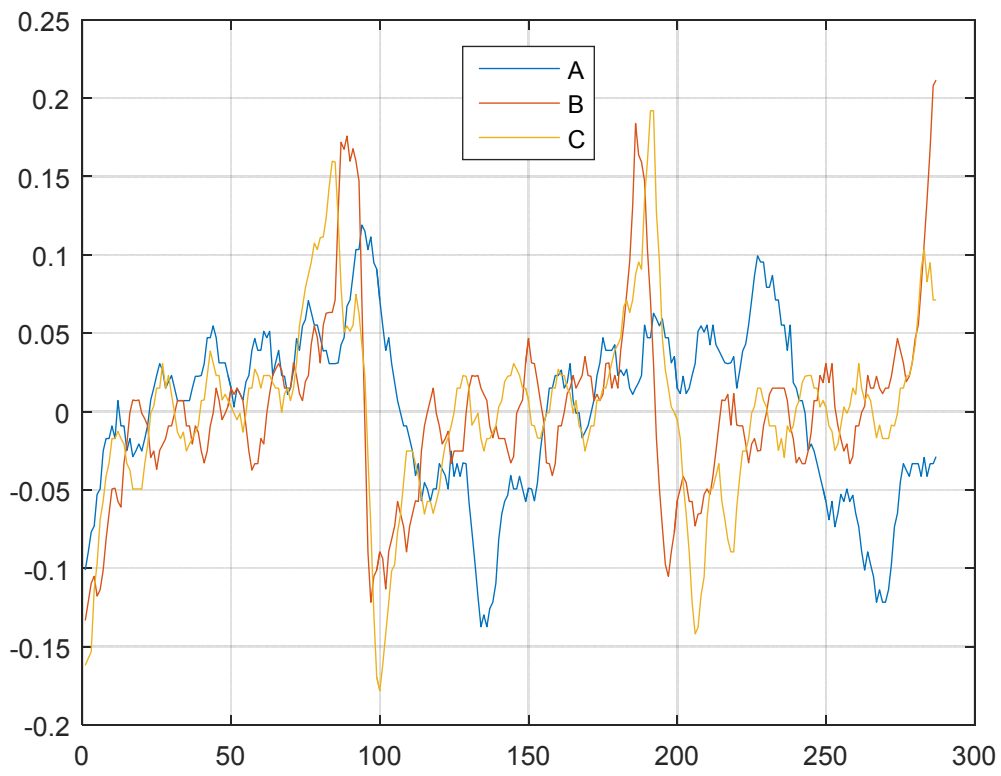


Fig 4.1.2.3. A signal matching graph applied correlation signal processing.

Correlation between different signals	Matching
Correlation with bump(A) and spike(B)	4%
Correlation between bump(A) with dome(C)	16%
Correlation between spike(B) with dome(C)	67%

Table 4.1.2.1. Correlation coefficients between bump, spike and dome signals.

4.2 Characteristics of Sliding Signals

We identified that sliding signals were different depending on texture shapes, so it was necessary to analyze a mechanism of the signal difference. Here, mechanism of sliding signals was demonstrated and characteristics of sliding signal were explained. In the previous experiments, sliding velocity and weight were constant as 30mm/s and 200g respectively but, sliding signals with various sliding velocity and weight conditions were measured in the section.

4.2.1 Signal Difference depending on Texture Shapes

Piezoelectricity is a property generating a voltage in response to external strains. In touch case, a piezoelectric signal normally has high positive peak and negative peak having a high slope, because a pressure was applied suddenly in a short time. However, an applied pressure is changed according as contact area and contact time under a sliding case. So, the piezoelectric signal of pressure and sliding should be different. Magnified sliding signals and a schematic expressing the sliding mechanism were indicated in the Fig 4.2.1.1. We divided the sliding signals as three parts to explain the mechanism. When a texture was moved forward a cell, the texture started to press the cell and a positive slope appeared as the result (Fig 4.2.1.1.a). After that, a positive peak appeared, when a texture is located in the center of the cell because the highest pressure was applied in this time (Fig 4.2.1.1.b). The applied pressure decreased, since the texture was away from the center of the cell and an occurred voltage also decreased according to the reduced pressure. After the texture passed the cell entirely, negative peak appeared to return to the neutral states (Fig 4.2.1.1.c). We found that the time interval between positive and negative peaks was different depending on textures. This difference was caused by a contact area of textures [55]. In a bump texture, the time interval was longest as

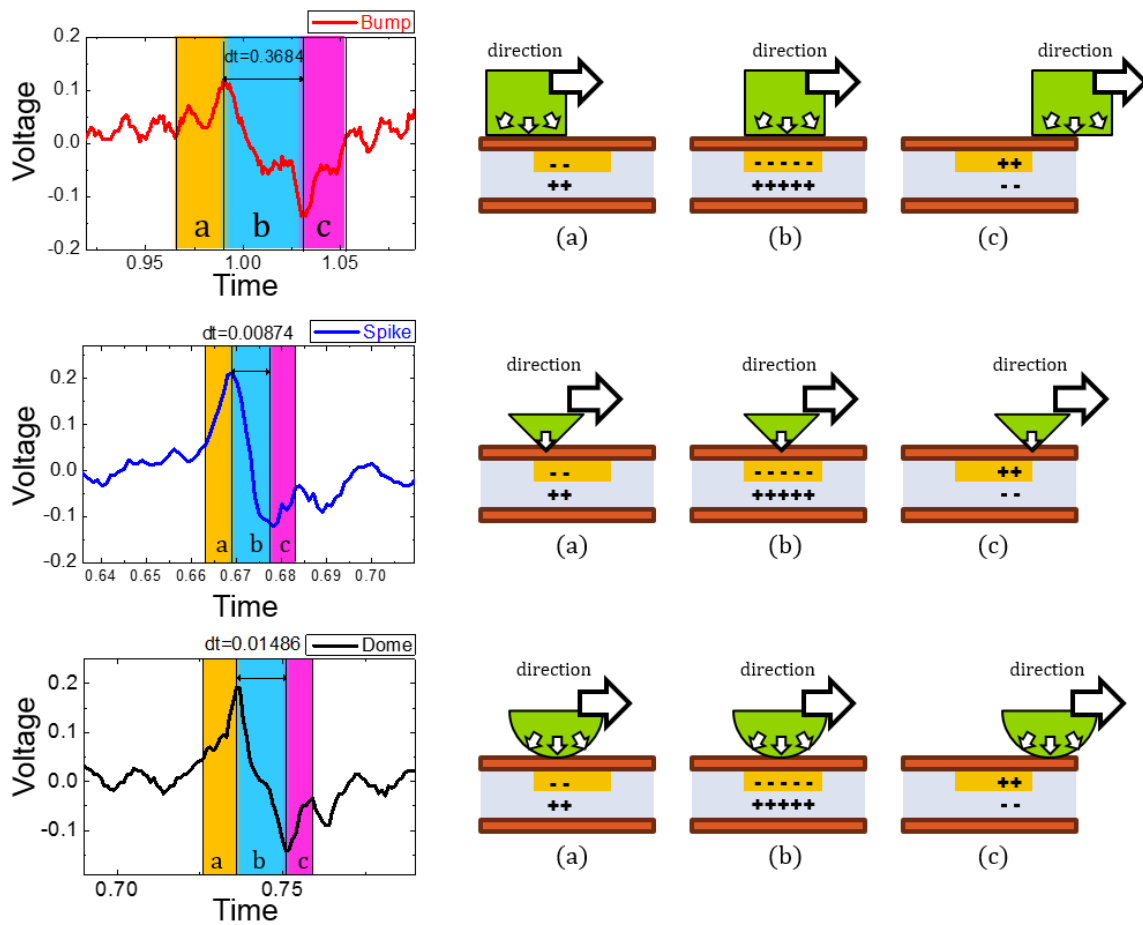


Fig 4.2.1.1. Sliding signal analysis in 30mm/s condition. (a) The cells were pressed when the texture was approached to the cell. In this moment, positive slope was occurred. (b) The highest pressure was applied to the cell, when the texture was located in the center of the cell. A positive peak appeared in this time. After that, as the texture was away from the cell, the applied pressure applied decreased. When the texture was get out of the cell entirely, a negative peak appeared. The difference of three sliding signals is the time interval between positive and negative peaks. The difference was derived from a contact area.

0.3684s because of its large contact area. However, spike texture had the shortest time interval as 0.0087s due to its small contact area. The dome texture had a middle time interval value as 0.1486s. We also could distinguish between bump and spike textures quantitatively as using this method, not by using signal wave form. However, it is hard to define texture's shape through the time interval differences because the interval values were related with texture's width.

4.2.2 Signal Difference depending on Weights

The 200g weight was used for the experiment so far. We also measured the sliding signal changes depending on the weight as 500g and 700g with the bump texture. The piezoelectricity makes a voltage corresponding to an applied pressure so, it generates more voltage under a heavy weight. The results also showed voltage increases in accordance with the heavy weights (Fig4.2.2.1.a). However, signal wave form was distorted as the weight increased. Also when heavy weight was used, the calculated velocity had some errors. Thus, the optimization is necessary for sliding experiments.

4.2.3 Signal Difference depending on Velocity

Here, we identified that there was a voltage difference according to velocity changes. The dome texture was used for this experiment. Piezoelectric voltage is related to a by

$$V_p = \frac{d_{33}}{e_{33}} \frac{t}{A} \cdot F ; \quad F = m \frac{dv}{dt} \quad (5)$$

where d_{33} and e_{33} are piezoelectric constants, t is thickness of piezoelectric material, A is an electrode area. The d_{33} , e_{33} , t and A are constants determined by material property and sensor design. Also applied weight was fixed as 200g, m is constant as well. However, the $\frac{dv}{dt}$ value in 70mm/s condition is much higher than 10mm/s condition, so high V_p appeared relatively. (Fig4.2.2.1.b). Sliding signals in slow velocity condition had low voltages and many noise as well as the signal wave form was ambiguous. Sliding signals of high velocity condition had clean signal form, but signals were also distorted as the velocity increased. Thus, it was necessary to optimize a velocity condition then, 30mm/s was chosen for the optimization.

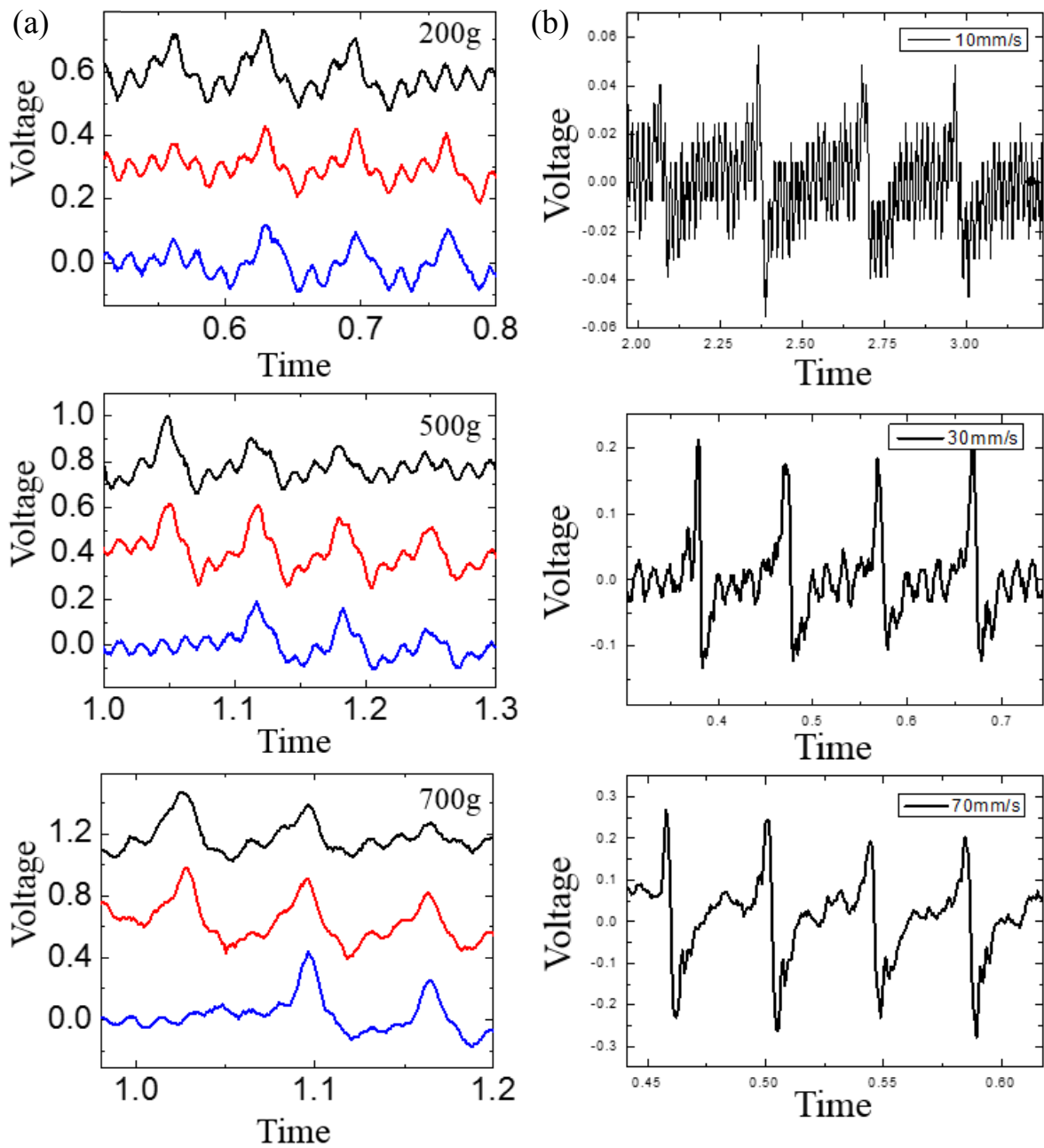


Fig 4.2.2.1. Sliding signal changes according to weight and velocity. (a) The output voltage increased according to weight in same velocity condition. (b) The output voltage increased according to weight in same s velocity condition.

4.3 Sliding velocity & Texture's Pitch Calculation

We confirmed that it is possible to distinguish between bump and spike textures through the previous experiment results. Here, we check whether the sensor can measure a sliding velocity.

Fig 4.3.1.a. indicates a successive sliding signals appeared in B and C cells and a schematic corresponding with the sliding condition. The sliding signal arisen from the B cell first and

then appeared in C cell in sequence, while the texture was moved. We could calculate a sliding velocity reversely by using the simple equation as

$$v = \frac{L}{T} \quad (6)$$

where T is a time interval of the sliding signals occurred from B and C cells and L is a distance between the two cells. L is fixed as 2mm and T is measured as 0.06644s (Fig 4.3.1.a). The calculated velocity was 30.1mm/s and the value was very close to a real sliding velocity of the linear stage. The reason the sensor could take a sliding velocity was that the sensor had the array structure. A unit sensor like a robotic finger is difficult to measure a sliding velocity by itself. In the robot filed, sliding velocity should be normally measured by adding a gyroscope or external circuit to the unit sensor. However, the sensor array consists of many cells and the distance between cells is always constant as 2mm. Thus, sliding velocity can be easily calculated in spite of an unknown velocity condition. So, the sensor array had a unique characteristic which can take a sliding velocity by itself without any additional equipment. We experimented the sliding velocity calculation in various conditions additionally. The sliding velocity of the linear stage was set as 10mm/s and 70mm/s respectively, and then we analyzed the occurred sliding signals to measure a sliding velocity reversely (Fig 4.3.1.b.c). The time intervals were 0.1826s and 0.02876s in 10mm/s and 70mm/s conditions respectively, and the calculated velocities were 10.95mm/s and 69.54mm/s by using (5). The result indicated that the sensor array can measure various sliding conditions. In addition, voltage differences were founded depending on velocity difference. Fig 4.3.1.d shows that the sensor could get a random velocity as well. In random velocity experiment, a texture was slid by the human instead of the linear stage so a sliding velocity was not constant but random. The time intervals were changed continuously from 0.05065s to 0.02870s corresponding to the random velocity. The calculated velocities were 40mm/s, 51mm/s, 57.5mm/s and 70mm/s respectively, so the sensor could even

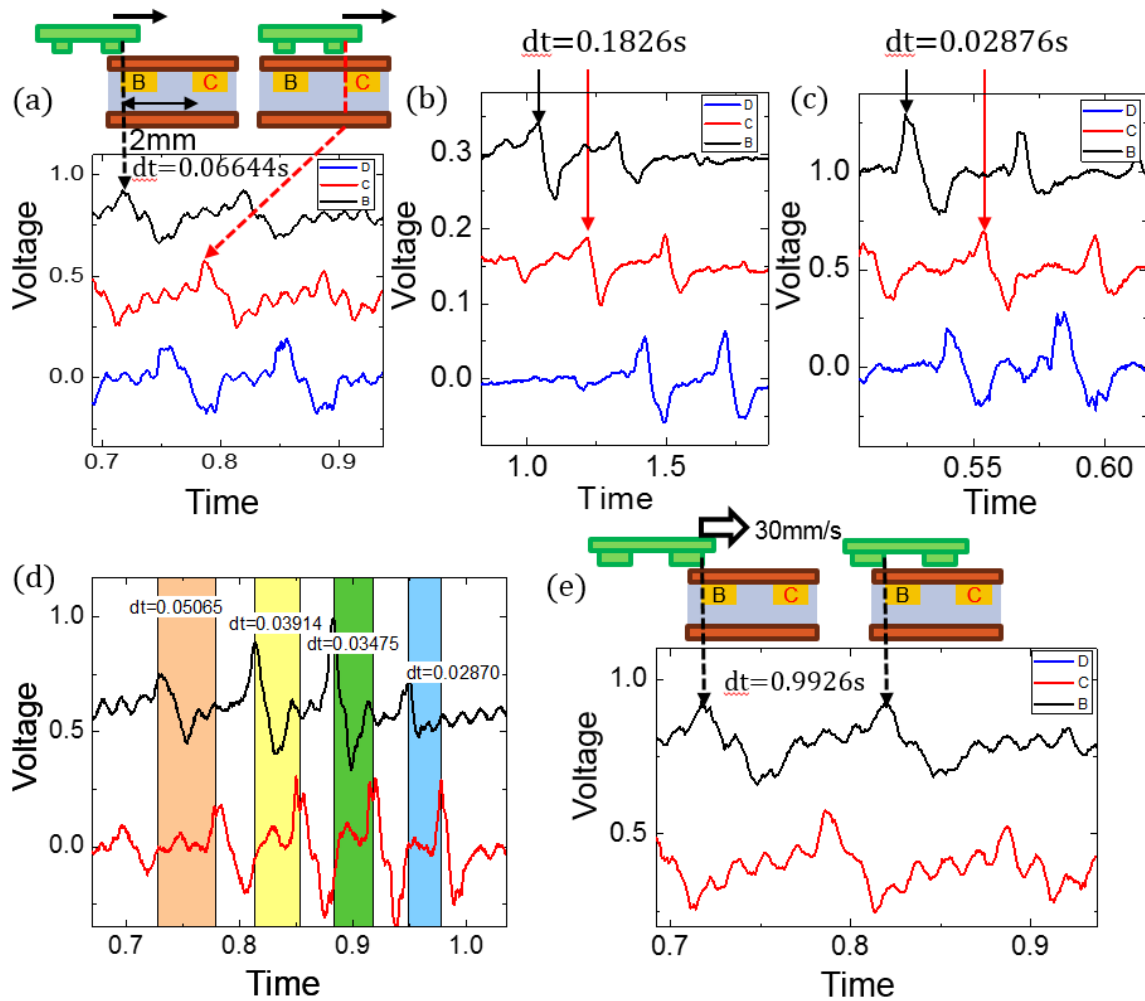


Fig 4.3.1. Velocity and pitch calculation processes using sliding signals. Sliding velocity could be calculated from consecutive sliding signals. (a) The mechanism of the velocity calculation. The time interval of sliding signals from B and C cells and distance between the two cells are used for the following equation (velocity=distance/time) and the calculated velocity is 30mm/s(0.06644s/2mm). (b), (c) The sensor array could measure the slow (10mm/s) and fast (70mm/s) conditions as well. (d) The sensor array could calculate a random velocity by using same calculation mechanism. (e) The pitch of texture calculation processes. The time interval of two sliding signals arisen from same cell and the calculated velocity were used for the following equation(distance=velocity*time) and the calculated distance was 3mm(30mm/s*0.9926s).

measure changing velocity. The ability allowed that the sensor can get acceleration as well. Furthermore, the sensor could also take a texture's pitch.

Fig 4.3.1.e is enlarged image of Fig 4.3.1.a and has a schematic corresponding with the bump texture sliding. The first bump texture passed B cell and then a second texture also passed the B cell during a sliding, so that the sliding signal appeared sequentially in the B cell. Thus, the time interval of the two sliding signals generated in the B cell was related with the texture's

pitch. We used the following equation to calculate the texture's pitch.

$$S = v \times T \quad (7)$$

The sliding velocity was set as 30mm/s as like before and a time interval of two signals was measured as 0.9926s. Texture's pitch could be calculated by multiplying velocity by time. The calculated pitch was 2.98mm. It was very close to an actual texture's pitch; 3mm. So, the sensor could measure both a sliding velocity and texture's pitch by itself.

4.4 Texture Restoration

We discussed the width of textures in the sliding signal mechanism section (Fig 4.2.1.1) and texture's pitch in sliding velocity calculation section (Fig 4.3.1) as well. Now, we will restore the texture structure by using the previous results. As we already mentioned, the time interval between positive and negative peaks is related with a contact area, that is, texture's width. First, row sliding signals changed to the absolute values to get the time interval more easily (Fig 4.4.1.) and then measured the time interval between two positive peaks. In bump texture, the time intervals were 0.3684s and 0.3813s. By using (7), texture's width also could be calculated as 1.1mm by multiplying 0.3684s by 30mm/s. The real width of bump texture is 1mm, so that the calculated bump width was very close to the actual width. The spike texture had the lowest time interval as 0.01s and 0.009s due to its small contact area and a calculated texture width was 0.3mm by using (7). However, a real texture width of spike texture was 0.15mm in spike texture so that there were some errors. A calculated width of the dome texture was 0.4mm by using (7). Originally, the dome texture should have small contact area because of its curved surface. However, 3D printed dome texture could not have perfect curved surface due to resolution problem of the 3D printer. The 3D printed dome texture had 0.4mm contact width in real and the contact width was close to the calculated texture width of the dome texture. We identified that texture widths of three different shapes can be calculated by using (7) and

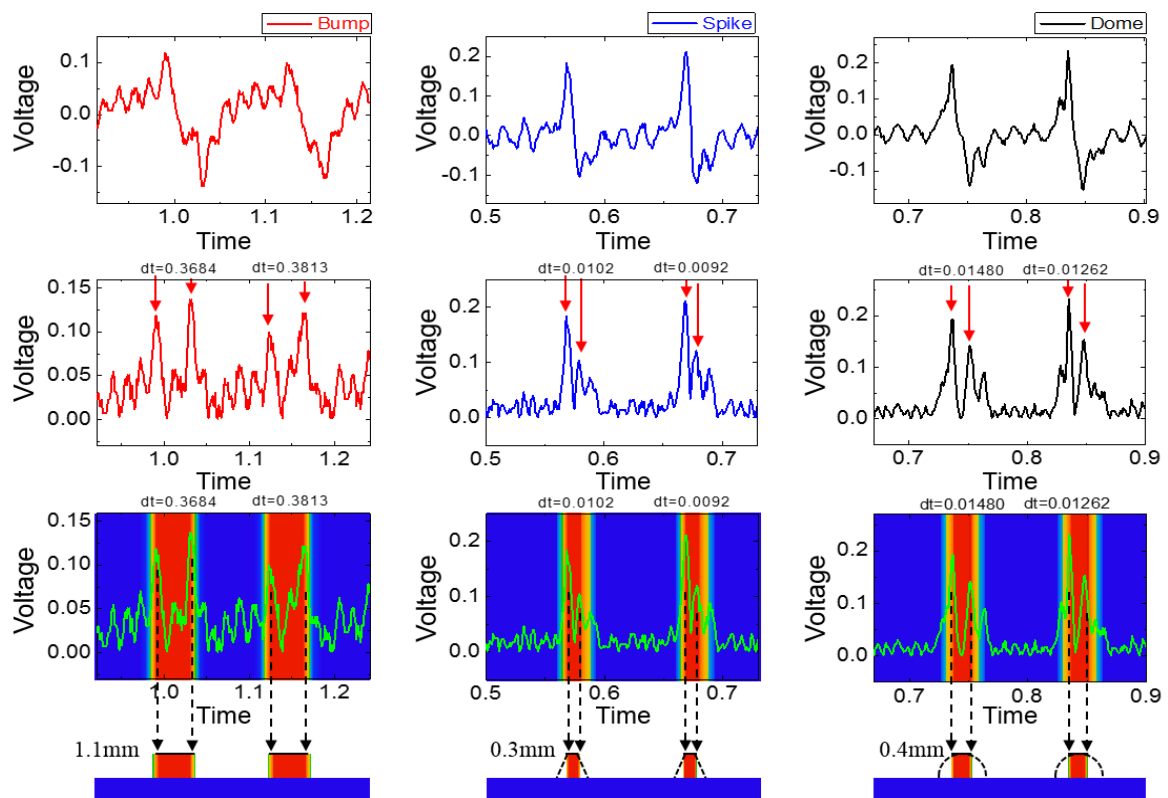


Fig 4.4.1. Texture restoration of the three different textures. The width of textures could be calculated by multiplying the time interval between positive and negative peaks and sliding velocity. The row sliding signal data changed to the absolute value for extracting time interval(dt) easily. The calculated width had good accuracy compared with real width. Texture's patterns were expressed as the color mapping. However, there are no information about z-axis information of the textures, so that it is hard to distinguish between a narrow bump and spike textures.

the calculated results were very closed to the actual width. The color mapping was applied to express texture's pattern as the red and blue color. Pressure and non-pressure areas were expressed by the red and blue color respectively. However, this calculation method could not deal with z-axis information because it is only related with contact areas. Thus, it should be confused to distinguish between 0.4mm bump texture with dome texture and there was still error problem in spike texture.

4.5 Resolution of the Piezo Sensor Array

We used textures having a 3mm pitch in common for pervious experiments so far. It was easy to measure the sliding signals from the sensor array, because the sensor had a high resolution than textures. So, the results of previous experiments are probably natural. Here, we will discuss about the sensor resolution. A spike texture having a 0.5mm pitch to 3mm at intervals of 0.5mm was slid on the sensor at 35mm/s. The result showed that an interval of the signals increased with the texture's pitch (Fig 4.5.1). It meant that the sensor could measure a high resolution condition than itself such as 0.5mm, 1mm and 1,5mm pitch conditions. The time intervals under higher resolution conditions were measured as 0.01564s, 0.03165s and 0.04609s and we analyzed that the results by multiplying a 35mm/s velocity. The calculated pitches were 0.54mm, 0.95mm and 1.54mm and it was close to actual texture's pitch accurately. So, we also checked that the sensor had a higher resolution characteristic than the sensor system.

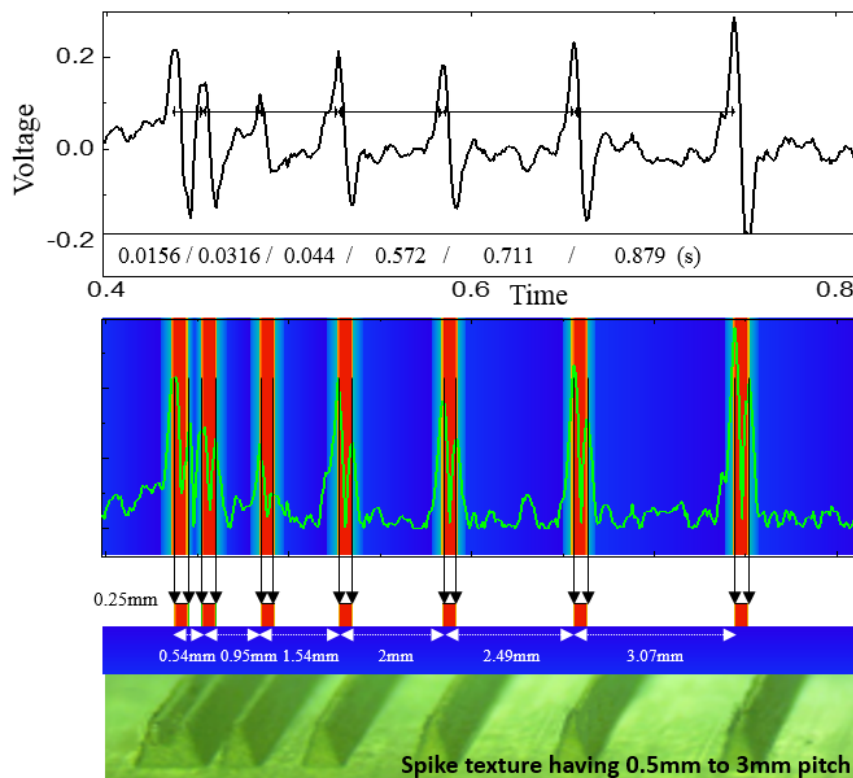


Fig 4.5.1. Sliding signal of random pitch in 35mm/s condition. The sensor could measure sliding signals having 0.5mm, 1mm and 1.5mm pitch although the sensor had 2mm pitch. The array sensor had a higher resolution than sensor system.

4.6 Characteristics of Piezo Sensor array applied Soft Material

Until now, we demonstrated how to measure sliding velocity, texture's pitch and width from analyzing the sliding signals. The sliding velocity and texture's pitch could be measured regardless of texture shapes. However, there were some errors to take the texture's width and distinguish between spike and dome textures. We thought that mimicking the human skin should be a key to solve this problem because the human distinguishes textures from their deformed skin. For example, the amount of a skin deformation is different depending on an

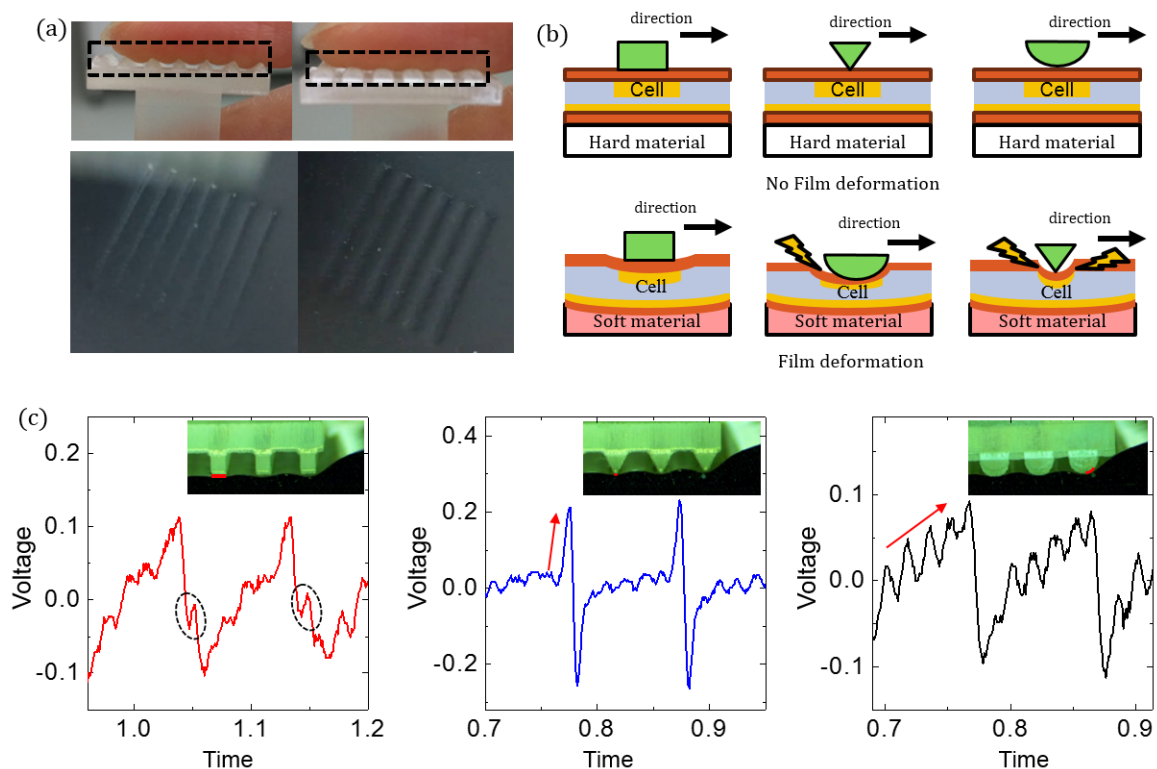


Fig 4.6.1.1. A deformation mechanism and signal changes after applying a soft material to the sensor. (a) Deformation differences depending on texture shapes at a skin and sponge. (b) In hard materials condition, sensor could not be deformed sufficiently. Contact areas and magnitude of deformation were changed corresponding with the textures in soft materials condition. The deformation induced changes of sliding signals wave form and output voltage. (c) Characteristics of sliding signals after applying a sponge layer. After sponge layer was applied the sensor array, each sliding signal could have a unique characteristic. Bump signal had a small noise between positive and negative peaks. Spike signal had very high slope and voltage. Dome signal had gradual slope due to smooth side.

applied pressure so, the human can distinguish between the spike and dome textures due to the pressure difference.

4.6.1 Sliding Signal Changes

In fig 4.6.1.1.a shows the deformation difference between spike and dome textures at a skin and sponge. Previous experiments were proceeded on hard materials like a desk. So the array sensor could not be deformed sufficiently. In hard material condition, both spike and dome textures had a small point contact with the sensor (Fig 4.6.1.1.b). That is, the reason the sliding signals of spike and dome textures were same was that both textures had small point contact with the array sensor, despite their real shapes were different.

A soft material was applied to the bottom of the sensor to induce a sensor deformation. After applying the soft material, the sliding signals of the three different textures could have unique characteristics respectively because of the sensor deformation (Fig 4.6.1.1.c). Small noises were found continuously between positive and negative peaks in the bump texture. The noise arisen from the uneven surface of the bump texture, because the bump texture had line contact with sensor during a sliding. In the spike texture, sliding signal of the spike texture had a low noise and clean signal shape than before. Also, there was no noise between two peaks due to its small contact area. Especially, output voltage was same as before. On the other hand, voltage and signal wave form were changed in the dome texture. The side of the dome texture pressed to the sensor with line contact during a sliding. And it also had a point contact with the sensor in the center of the dome texture. It meant that the dome texture had both line and point contact with the sensor. This characteristic appeared in a sliding signal of the dome texture very well. A gradual slope having many noise (red arrow) was induced by an uneven side of the dome texture during line contacting. No-noise areas between the two peaks indicated that it has a point contact like the spike texture. Besides, decreased voltage also could be a proof

that the dome texture has a line contact. Now we could distinguish the three textures through their unique characteristics of the sliding signals. The characteristics came from a sensor deformation, so that applying a soft material could be an effective solution for the tactile sensors.

4.6.2 Texture Restoration

After applying a soft material to the sensor, we restored the structure of texture again. The sliding signals occurred by three different textures were analyzed to measure a width of a textures by using the same signal processing. The calculated widths of the three textures had more accuracy than before. The error of the spike texture was reduced 0.3mm to 0.2mm in particular and it was really close to a real width as 0.15mm (Fig 4.6.2.1). A calculated width of the bump texture also perfectly same with a real width as 1mm. There was a difference in a

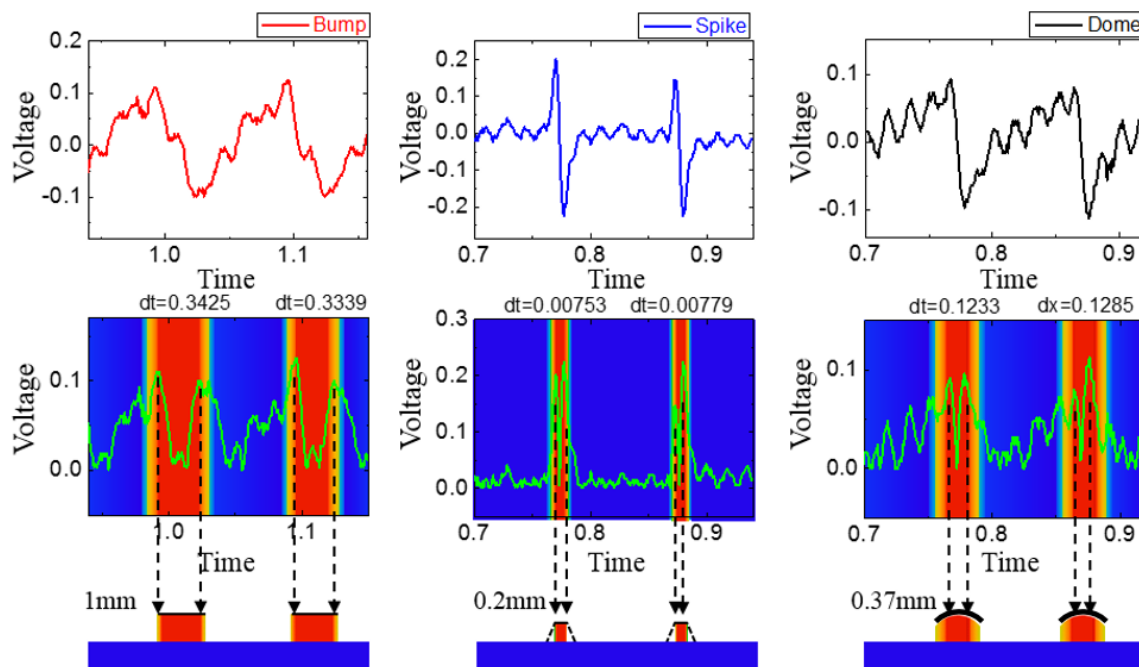


Fig 4.6.2.1. Texture restoration applied a soft material. The sliding signal data was changed to the absolute value for extracting time interval(dt) easily. The results were more accurate than non-soft material condition. Especially the width error decreased in the spike texture. The color mapped images had a z-axis information due to the soft material.

color mapping as well. Especially, pressure arisen from the side of the dome texture could be expressed by the color mapping as to its gradual slope. Applying a soft material brought not only a low error rate than before but also z-axis information.

IV. CONCLUSION

In summary, we proposed a tactile sensor which can take a normal pressure, sliding velocity, texture's pitch and width and texture's shapes by using simple signal processing through sliding experiments. In addition, the sensor had a higher resolution than sensor system. PVDF-TrFE which one of the popular piezoelectric copolymer was used for the piezo sensor array to measure a dynamic movement like a sliding because of its fast response and high sensitivity. The piezoelectric copolymer material allowed that the sensor could have a flexibility, easy-fabrication and self-bias characteristics. A soft material was applied the piezo sensor array for mimicking the human skin. The flexible substrate and soft material made the piezo sensor array deform while sliding experiments and those allowed that the sliding signal have unique characteristics. Because of the sensor deformation, each sliding signal corresponding with bump, spike and dome textures had different characteristics respectively. It allowed the sensor can distinguish texture's shape and detect texture's width accurately. The sliding velocity and texture's pitch are obtained by analyzing the signals derive from array cells. A simple calculation and signal processing was used for calculating the velocity and pitch. Surface textures were restored by using the previously calculated velocity and pitch values. Restored surface textures had high accuracy compared with real texture structures and color mapping was applied the restored textures images to express the texture's pattern. However, it was hard to restore a z-axis information. However, there were challenges for complex texture's shape detection, because the array sensor could not measure z-axis information precisely. The capabilities of velocity detecting and texture restoration allow the sensor can be utilized to electro-mechanical systems as the physical and the psychological tactile sensor.

Reference

- [1] A. Chortos, J. Liu, and Z. Bao, "Pursuing prosthetic electronic skin," *Nature Materials*, vol. 15, pp. 937-950, 2016.
- [2] M. Di Donato, "Development of composite piezoelectric materials for tactile sensing," Politecnico di Torino, 2015.
- [3] C. Metzger, E. Fleisch, J. Meyer, M. Dansachmüller, I. Graz, M. Kaltenbrunner, *et al.*, "Flexible-foam-based capacitive sensor arrays for object detection at low cost," *Applied Physics Letters*, vol. 92, p. 013506, 2008.
- [4] D. J. Lipomi, M. Vosgueritchian, B. C. Tee, S. L. Hellstrom, J. A. Lee, C. H. Fox, *et al.*, "Skin-like pressure and strain sensors based on transparent elastic films of carbon nanotubes," *Nature nanotechnology*, vol. 6, pp. 788-792, 2011.
- [5] Y. Huang, H. Yuan, W. Kan, X. Guo, C. Liu, and P. Liu, "A flexible three-axial capacitive tactile sensor with multilayered dielectric for artificial skin applications," *Microsystem Technologies*, pp. 1-6.
- [6] Y. Jeong, M. Sim, J. H. Shin, J.-W. Choi, J. I. Sohn, S. N. Cha, *et al.*, "Psychological tactile sensor structure based on piezoelectric nanowire cell arrays," *RSC Advances*, vol. 5, pp. 40363-40368, 2015.
- [7] C. Li, P.-M. Wu, S. Lee, A. Gorton, M. J. Schulz, and C. H. Ahn, "Flexible dome and bump shape piezoelectric tactile sensors using PVDF-TrFE copolymer," *Journal of Microelectromechanical Systems*, vol. 17, pp. 334-341, 2008.
- [8] D.-I. Kim, T. Q. Trung, B.-U. Hwang, J.-S. Kim, S. Jeon, J. Bae, *et al.*, "A Sensor Array Using Multi-functional Field-effect Transistors with Ultrahigh Sensitivity and Precision for Bio-monitoring," *Scientific reports*, vol. 5, 2015.
- [9] N. Thanh-Vinh, N. Binh-Khiem, H. Takahashi, K. Matsumoto, and I. Shimoyama, "High-sensitivity triaxial tactile sensor with elastic microstructures pressing on piezoresistive cantilevers," *Sensors and Actuators A: Physical*, vol. 215, pp. 167-175, 2014.
- [10] J. Park, M. Kim, Y. Lee, H. S. Lee, and H. Ko, "Fingertip skin-inspired microstructured ferroelectric skins discriminate static/dynamic pressure and temperature stimuli," *Science advances*, vol. 1, p. e1500661, 2015.
- [11] N. T. Tien, Y. G. Seol, L. H. A. Dao, H. Y. Noh, and N. E. Lee, "Utilizing highly crystalline pyroelectric material as functional gate dielectric in organic thin-film transistors," *Advanced Materials*, vol. 21, pp. 910-915, 2009.
- [12] N. T. Tien, S. Jeon, D. I. Kim, T. Q. Trung, M. Jang, B. U. Hwang, *et al.*, "A flexible bimodal sensor array for simultaneous sensing of pressure and temperature," *Advanced Materials*, vol. 26, pp. 796-804, 2014.
- [13] J. Platkiewicz, H. Lipson, and V. Hayward, "Haptic Edge Detection Through Shear," *Scientific reports*, vol. 6, 2016.
- [14] M. Kaneko and K. Tanie, "Contact point detection for grasping an unknown object using self-posture changeability," *IEEE Transactions on Robotics and Automation*, vol. 10, pp. 355-367, 1994.
- [15] A. J. Schmid, N. Gorges, D. Goger, and H. Worn, "Opening a door with a humanoid robot using multi-sensory tactile feedback," in *Robotics and Automation, 2008. ICRA 2008. IEEE International Conference on*, 2008, pp. 285-291.
- [16] A. A. Stanley, K. Hata, and A. M. Okamura, "Closed-loop shape control of a haptic jamming deformable surface," in *Robotics and Automation (ICRA), 2016 IEEE International Conference on*, 2016, pp. 2718-2724.
- [17] K. Suwanratchatamane, M. Matsumoto, and S. Hashimoto, "Robotic tactile sensor

- system and applications," *IEEE Transactions on Industrial Electronics*, vol. 57, pp. 1074-1087, 2010.
- [18] S. Dragiev, M. Toussaint, and M. Gienger, "Uncertainty aware grasping and tactile exploration," in *Robotics and Automation (ICRA), 2013 IEEE International Conference on*, 2013, pp. 113-119.
- [19] V. Maheshwari and R. F. Saraf, "High-resolution thin-film device to sense texture by touch," *Science*, vol. 312, pp. 1501-1504, 2006.
- [20] H. Yamazaki, M. Nishiyama, and K. Watanabe, "A hemispheric hetero-core fiber optic tactile sensor for texture and hardness detection," in *SPIE OPTO*, 2016, pp. 97540X-97540X-6.
- [21] S. Yun, S. Park, B. Park, Y. Kim, S. K. Park, S. Nam, *et al.*, "Polymer-Waveguide-Based Flexible Tactile Sensor Array for Dynamic Response," *Advanced Materials*, vol. 26, pp. 4474-4480, 2014.
- [22] A.-V. Ho and S. Hirai, *Mechanics of Localized Slippage in Tactile Sensing: And Application to Soft Sensing Systems* vol. 99: Springer, 2013.
- [23] H. Hu, Y. Han, A. Song, S. Chen, C. Wang, and Z. Wang, "A finger-shaped tactile sensor for fabric surfaces evaluation by 2-dimensional active sliding touch," *Sensors*, vol. 14, pp. 4899-4913, 2014.
- [24] D. Xu, G. E. Loeb, and J. A. Fishel, "Tactile identification of objects using Bayesian exploration," in *Robotics and Automation (ICRA), 2013 IEEE International Conference on*, 2013, pp. 3056-3061.
- [25] R. S. Dahiya, G. Metta, M. Valle, and G. Sandini, "Tactile sensing—from humans to humanoids," *IEEE Transactions on Robotics*, vol. 26, pp. 1-20, 2010.
- [26] P. Delmas, J. Hao, and L. Rodat-Despoix, "Molecular mechanisms of mechanotransduction in mammalian sensory neurons," *Nature Reviews Neuroscience*, vol. 12, pp. 139-153, 2011.
- [27] R. S. Dahiya and M. Valle, *Robotic tactile sensing: technologies and system*: Springer Science & Business Media, 2012.
- [28] H. Liu, X. Song, T. Nanayakkara, K. Althoefer, and L. Seneviratne, "Friction estimation based object surface classification for intelligent manipulation," in *IEEE International Conference on Robotics and Automation*, 2011.
- [29] A. Spiers, M. Liarokapis, B. Calli, and A. Dollar, "Single-Grasp Object Classification and Feature Extraction with Simple Robot Hands and Tactile Sensors."
- [30] A. Naceri, M. Santello, A. Moscatelli, and M. O. Ernst, "Digit Position and Force Synergies During Unconstrained Grasping," in *Human and Robot Hands*, ed: Springer, 2016, pp. 29-40.
- [31] A. Moringen, R. Haschke, and H. Ritter, "Search procedures during haptic search in an unstructured 3D display," in *2016 IEEE Haptics Symposium (HAPTICS)*, 2016, pp. 192-197.
- [32] N. Kawasegi, J. Sumioka, N. Takano, S. Yamada, and M. Fujii, "The microtextured plastic moldings to control human tactile sense: The texture effect enhancement due to apical shape and material frictional properties," *Precision Engineering*, vol. 45, pp. 126-135, 2016.
- [33] X. Song, H. Liu, J. Bimbo, K. Althoefer, and L. D. Seneviratne, "Object surface classification based on friction properties for intelligent robotic hands," in *World Automation Congress (WAC), 2012*, 2012, pp. 1-5.
- [34] M. Gee, P. Tomlins, A. Calver, R. Darling, and M. Rides, "A new friction measurement system for the frictional component of touch," *Wear*, vol. 259, pp. 1437-1442, 2005.
- [35] W. Yang, G. Gu, X. Zhou, F. Xu, and K. Ren, "The estimation of surface roughness

- with the utilization of Mueller matrix," *Infrared Physics & Technology*, vol. 76, pp. 748-755, 2016.
- [36] K. Nemoto, K. Yanagi, M. Aketagawa, I. Yoshida, M. Uchidate, T. Miyaguchi, *et al.*, "Development of a roughness measurement standard with irregular surface topography for improving 3D surface texture measurement," *Measurement Science and Technology*, vol. 20, p. 084023, 2009.
- [37] J. A. Fishel, V. J. Santos, and G. E. Loeb, "A robust micro-vibration sensor for biomimetic fingertips," pp. 659-663.
- [38] N. Jamali and C. Sammut, "Material classification by tactile sensing using surface textures," pp. 2336-2341.
- [39] Z. Liao, W. Liu, Y. Wu, C. Zhang, Y. Zhang, X. Wang, *et al.*, "A tactile sensor translating texture and sliding motion information into electrical pulses," *Nanoscale*, vol. 7, pp. 10801-10806, 2015.
- [40] A. Yu, P. Jiang, and Z. L. Wang, "Nanogenerator as self-powered vibration sensor," *Nano Energy*, vol. 1, pp. 418-423, 2012.
- [41] T. Iwasaki, T. Takeshita, Y. Arinaga, K. Uemura, H. Ando, S. Takeuchi, *et al.*, "Shearing force measurement device with a built-in integrated micro displacement sensor," *Sensors and Actuators A: Physical*, vol. 221, pp. 1-8, 2015.
- [42] C. Pan, L. Dong, G. Zhu, S. Niu, R. Yu, Q. Yang, *et al.*, "High-resolution electroluminescent imaging of pressure distribution using a piezoelectric nanowire LED array," *Nature Photonics*, vol. 7, pp. 752-758, 2013.
- [43] S. Chun, Y. Kim, H.-S. Oh, G. Bae, and W. Park, "A highly sensitive pressure sensor using a double-layered graphene structure for tactile sensing," *Nanoscale*, vol. 7, pp. 11652-11659, 2015.
- [44] M. L. Hammock, A. Chortos, B. C. K. Tee, J. B. H. Tok, and Z. Bao, "25th Anniversary Article: The Evolution of Electronic Skin (E-Skin): A Brief History, Design Considerations, and Recent Progress," *Advanced Materials*, vol. 25, pp. 5997-6038, 2013.
- [45] J. Tichy, J. Erhart, and E. Kittinger, *Fundamentals of piezoelectric sensorics*: Springer, 2010.
- [46] M. Ha, S. Lim, J. Park, D. S. Um, Y. Lee, and H. Ko, "Bioinspired Interlocked and Hierarchical Design of ZnO Nanowire Arrays for Static and Dynamic Pressure-Sensitive Electronic Skins," *Advanced Functional Materials*, vol. 25, pp. 2841-2849, 2015.
- [47] M. Di Donato, "Development of composite piezoelectric materials for tactile sensing," 2015.
- [48] K. Uchino and K. Uchino, "The development of piezoelectric materials and the new perspective," *Advanced piezoelectric materials-science and technology. Padstow, Cornwall: Woodhead Publishing*, pp. 1-43, 2010.
- [49] K. Xi, Y. Wang, D. Mei, G. Liang, and Z. Chen, "A flexible tactile sensor array based on pressure conductive rubber for three-axis force and slip detection," in *2015 IEEE International Conference on Advanced Intelligent Mechatronics (AIM)*, 2015, pp. 476-481.
- [50] S. Y. Kim, S. Park, H. W. Park, D. H. Park, Y. Jeong, and D. H. Kim, "Highly Sensitive and Multimodal All-Carbon Skin Sensors Capable of Simultaneously Detecting Tactile and Biological Stimuli," *Advanced Materials*, vol. 27, pp. 4178-4185, 2015.
- [51] C.-W. Ma, T.-H. Lin, and Y.-J. Yang, "Tunneling piezoresistive tactile sensing array fabricated by a novel fabrication process with membrane filters," in *2015 28th IEEE International Conference on Micro Electro Mechanical Systems (MEMS)*, 2015, pp.

- 249-252.
- [52] H.-K. Lee, J. Chung, S.-I. Chang, and E. Yoon, "Normal and shear force measurement using a flexible polymer tactile sensor with embedded multiple capacitors," *Journal of Microelectromechanical Systems*, vol. 17, pp. 934-942, 2008.
 - [53] L. Viry, A. Levi, M. Totaro, A. Mondini, V. Mattoli, B. Mazzolai, *et al.*, "Flexible three-axial force sensor for soft and highly sensitive artificial touch," *Advanced Materials*, vol. 26, pp. 2659-2664, 2014.
 - [54] M. Mukaka, "A guide to appropriate use of Correlation coefficient in medical research," *Malawi Medical Journal*, vol. 24, pp. 69-71.
 - [55] J. Song, X. Wang, J. Liu, H. Liu, Y. Li, and Z. L. Wang, "Piezoelectric potential output from ZnO nanowire functionalized with p-type oligomer," *Nano letters*, vol. 8, pp. 203-207, 2008.
 - [56] https://en.wikipedia.org/wiki/Somatosensory_system
 - [57] https://en.wikipedia.org/wiki/Sensory_receptor
 - [58] https://en.wikipedia.org/wiki/Surface_finish
 - [59] <https://en.wikipedia.org/wiki/Piezoelectricity>
 - [60] <https://en.wikipedia.org/wiki/Array>
 - [61] https://en.wikipedia.org/wiki/Correlation_and_dependence
 - [62] http://students.asl.ethz.ch/upl_pdf/231-report.pdf, 'Force sensing technologies,'

요 약 문

표면 형태 감지를 위한 정신감각적 촉각 센서 구조 연구

예전부터 사람의 오감은 매우 흥미로운 학문이었다. 특히 시각과 청각은 오래전부터 연구돼 왔으며 그 결과로 사람의 시각을 모방한 카메라와 청각을 모방한 마이크가 개발됐다. 최근 들어서는 사람의 촉각을 모방하는 기술이 많이 연구되고 있다. 대표적으로 다양한 물질을 사용하여 압력, 온도, 진동을 감지하는 촉각감지 기술들이 많이 연구됐다. 또한 사람의 피부처럼 늘어나고 구부러질 수 있는 플렉서블한 특성과 심지어 스티커처럼 특정 물체에 접착이 가능한 센서도 개발되고 있다. 하지만 아직까지 촉각 센서들이 사람의 촉각을 완전하게 모방하지 못하고 있다. 촉각은 온도 압력 진동 감지 외에도 거칠기, 부드러움, 딱딱함, 형태 구분 등 정신 감각적인 파라미터들도 느끼기 때문이다. 실제로 사람의 촉각 시스템에는 여러 종류의 촉각기관들이 존재하며, 이 많은 촉각 수용기들이 피부 속에 매우 밀집하게 존재하기 때문에 사람이 다양한 촉각을 동시에 느낄 수 있다. 더군다나 정신 감각적인 요소들은 사람마다 기준이 다르므로 이를 연구하기 위해서는 많은 이슈가 있고, 그래서 상대적으로 정신 감각적 요소 중 하나인 표면의 형태를 구별해내는 센서는 많이 연구된 바가 없다. 로봇 분야에서 로봇 손가락에 피드백 루프나 플로차트를 이용하여 표면의 거칠기와 물체의 모형을 알아내는 연구가 진행되고 있다. 하지만 이런 로봇 손가락으로부터 표면 형태를 구하려면 로봇손가락을 위한 부수적인 장치와 복잡한 알고리즘이 필수적이라는 단점이 있다. 그 외에도 또한 빛을 광학적 특성이나 piezophotonic 물질을 이용하여 표면 형태를 감지하는 연구들이 있지만, 전원 및 광원 공급과 부수적인 광학장비들의 필수라는 단점들이 있다. 이 논문에서는 압전물질과 부드러운 물질을 적용한 센서로 압력을 구할 수 있을 뿐만 아니라 특정 형태와 센서를 슬라이딩함으로써 표면의 형태를 복원하는 것을 다룰 것이다. 표면 형태 복원을 위하여 간단한 신호처리가 사용되었으나, 로봇 분야와는 다르게 추가적인 장치 없이 센서 자체만으로 슬라이딩 속도를 역산해 낼 수 있고, 형태를 복원할 수 있는 특징이 있다. 또한, 어레이 구조를 적용해 높은 해상도를 가지고 있다. 이런 특징으로부터 촉각 센서가 압력과 온도 같은 정량적인 것을 측정할 수 있는 것에서 벗어나, 정신 감각적인 분야에 좀 더 다가갈 수 있는 의미를 가질 수 있다. 또한, 센서 분야에서도 단순 신호처리를 이용하여 표면의 특징을 잡아낼 수 있다는 의미가 있다.

키워드 : 피에조센서, 어레이 구조, 정신감각적, 표면형태,